June 2018

Stormwater Inputs in Urban Streams: Impact and Persistence of Effects on Stream Temperature

Samuel Harrison Caldwell
Syracuse University

Abstract

Stream temperature is an important metric for determining the health of a stream system, and derived from complex interactions between climate, weather, and local landscape characteristics. In urban areas, stream temperature is additionally influenced by impervious surfaces as well as stormwater infrastructure that translates water quickly to stream channels. Disentangling the impacts of spatial and temporal drivers of the stream temperature regime is therefore a complex task. To improve understanding of spatial and temporal variability in stream temperatures, we combined in situ stream temperature loggers with thermal infrared (TIR) imagery collected via unmanned aerial vehicles (UAV) along a 2.25 km section of creek in Syracuse, NY. TIR imagery was used document the heterogeneity of stream temperature as impacted by a natural spring and several stormwater inputs across the stream channel and down the length of a stream for three flights in May, June, and July of 2017. Thermal heterogeneities derived from stormwater culverts were observed to persist as far as 290 m downstream from their source depending on the time of year. Reach observations and weather station data were combined with TIR imagery to calibrate a deterministic stream temperature model using a modified version of HFLUX 3.0. Stream temperatures were simulated in HFLUX for a five-day period, after a two day warm up, surrounding monthly flights using different combinations of stormwater discharge and temperature. The use of two metrics derived from the TIR data, an 'Initial Impact' (on stream temperature) and 'Effect Duration', enabled spatial model calibration alongside temporal calibration to iButton observations at the end of the reach. Discrepancies between best models fits through space and best model fits through time establish that model approaches should incorporate errors in multiple dimensions. Overall, this study demonstrates that stormwater inputs in northeastern watersheds may cool mean stream temperatures, with effects that can persist for hundreds of meters downstream. Beyond the impact of stormwater, we also show that UAV-based TIR can be particularly useful for documenting these impacts when paired with in situ sensors. Finally, we find that calibrating models in multiple dimensions can more accurately simulate spatio-temporal hydrologic processes and mixing between urban water sources and the main channel.

Stormwater Inputs in Urban Streams: Impact and Persistence of Effects on Stream Temperature

By

Samuel Caldwell

B.A. Amherst College, Amherst, MA, 2016

Thesis

Submitted in partial fulfillment of the requirements for the degree of

Master of Science in *Earth Sciences*

Syracuse University

June 2018

Table of Contents

List of Figures

1 Introduction

Stream temperature is an important environmental variable and measure of water quality (Likens et al., 1969; Schindler, 2001; Caissie, 2006; Whitehead et al., 2009). A stream's temperature regime broadly influences many processes, including nutrient cycling and the concentrations of solutes (LeBosquet et al., 1950; Poole & Cara, 2001). Stream temperature also impacts the activity of many organisms living within the stream channel and in the surrounding benthos (e.g., Allen, 1995; Holtby 1988; Olden, 2010). Given its connections with dissolved oxygen, nutrient cycling, and biotic processes, stream temperature can also be a proxy for overall stream health (Likens et al., 1969; Schindler, 2001; Caissie, 2006; Whitehead et al., 2009). Finally, stream temperature helps to identify discrete and diffuse sources of water to the stream channel, and the impact of those sources on temperature heterogeneity within a stream (Lautz, 2012; Irvine et al., 2015; Irvine et al., 2016; Dugdale et al., 2016).

In pursuit of understanding the spatio-temporal behavior of stream temperature, controls on the stream temperature regime in a myriad of systems have been extensively studied and well documented (Caissie, 2006; Webb et al., 2008). Broadly, landscape characteristics and atmospheric drivers determine and influence spatio-temporal variations in heat fluxes, with the balance of these fluxes determining stream temperature. Atmospheric drivers, such as air temperature and short and longwave radiation, affect changes in temperature through time, while landscape characteristics often lead to spatial stream temperature variations. Landscape characteristics that may affect stream temperature include bedrock properties (Caissie, 2006), density and occurrence of a riparian buffer (Caissie, 2006; Somers et al., 2013; Garner et al., 2014), topographic shading (Caissie, 2006; Webb, 2008; Somers et al., 2013), and stream discharge and groundwater contribution (Caissie 2096; Kelleher et al. 2012).

Within urban systems, thermal pollution is often a concern, given the high concentration of impervious surfaces that are typically several degrees warmer than air temperatures (Herb et al., 2008; Somers et al., 2013). Studies have found elevated stream temperatures in urban as compared to nearby forested systems during baseflow (Somers et al., 2013), and have shown stream temperatures typically spike immediately after summer rain events, as impervious surfaces warm stormwater runoff contributing to urban stream channels. Stormwater infrastructure also translates runoff quickly to the stream channel (Walsh, 2005; Herb et al.,

2008; Somers et al., 2013). While the hydrology of urban stream systems is well documented (Wang et al., 2003; Walsh, 2005; Herb et al., 2008; Wenger et al., 2009; Somers et al., 2013; Booth et al., 2014; Zieger and Hubbart, 2015), the interplay between stormwater and stream temperature is less studied, as well as how these signals may propagate downstream. Existing work that has considered urban stream temperature heat budgets have focused on the propagation of heat to stormwater management ponds (Sabouri et al., 2017) as well as the moderating effects of riparian buffers on urban stream temperature (Beschta, 1997; Ghermandi et al., 2009). Additionally, heat budgets have been used in stream temperature models to determine groundwater contribution to streams (Glose et al., 2017) and predict stream temperature change as result of a given type, amount, and locale of urbanization (LeBlanc et al., 1996). Though a few studies of longitudinal variations in stream temperature exist in the literature (Fullerton et al., 2015; Schmadel et al., 2014), propagation of heat within urban systems is less studied.

One area of emerging research that is improving understanding of spatio-temporal stream temperatures is the use of unoccupied aerial vehicles (UAVs) to collect spatially distributed stream temperature observations via thermal infrared (TIR) cameras. This provides the opportunity to capture high resolution, two-dimensional spatial and temporal data along a given stream, useful for identifying points of homogeneity and heterogeneity (Dugdale, 2016). Knowledge of this spatial heterogeneity is critical to informing and improving stream temperature models, as well as refining conceptual models of urban stream temperatures and how they are impacted by stormwater hydrology. Thermal infrared imaging has been used for measuring water temperature since the 1970s and has become an increasingly popular tool for studying water temperature in part due to the ever-increasing quality of TIR cameras and the data they collect (Dugdale, 2016). Most studies of stream temperature use satellite, airplane or helicopter-deployed TIR cameras. While satellite or airbourne cameras are generally cooled thermal detectors if deployed by air, or photon detectors when deployed by satellite (Bhan et al., 2009), UAV TIR cameras are limited by payload capacity to uncooled microbolometers (Bhan et al., 2009; Dugdale, 2016; Lee et al., 2016). These cameras are smaller, relatively less expensive, and require less energy to run than their cooled counterparts (Bhan et al., 2009). Uncooled systems, while rapidly improving, have lower sensitivity and reliability of temperature detection than cooled systems (Niklaus, 2008; Bhan et al., 2009), and ongoing work seeks to demonstrate the utility of these systems to quantify spatio-temporal stream temperature at the

stream reach scale. To date, there are a few studies have shown the utility of UAVs to obtain aerial TIR for observing water temperatures (Jensen et al., 2012; Liu et al., 2015; Rautio et al., 2015; Lee et al. 2016). These studies have shown UAVs to be a reliable way to obtain TIR data at the reach-scale, with the scale of measurements determined by limitations in UAV flight times and federal law (Dugdale, 2016).

In this study, we employed in situ observations and novel data collection techniques via TIR imagery collected via UAV to study the impacts of urban stormwater on stream temperature. This study focuses on Onondaga Creek, a large urban stream in Syracuse, NY, to determine the effect, if any, of artificially channelized stormwater inputs to an urban stream. We first characterize temperature responses using in situ temperature sensors to measure stream temperature at the beginning and end of the reach followed by TIR surveys of the study area. Surveys were then paired with a modified version of the HFLUX model (Glose et al., 2017), a deterministic stream temperature model developed to quantify the ground water contribution to a stream based off of a heat budget analysis. Within this system, we used heat as a tracer to identify sources or sinks of heat to and from the stream channel (Lautz, 2012; Irvine et al., 2015; Irvine et al., 2016), quantifying the impact of stormwater discharge and temperature on stream temperature behavior. Overall, we aim to assess the potential of paired in situ and UAV-based TIR to characterize high spatial and high temporal resolution stream temperature response along a creek with stormwater impacts as well as how best to simulate and validate stormwater impacts using novel data sources.

2 Study Area

The study area consists of an approximately 2.25 km stretch of Onondaga Creek, located in Syracuse, NY. The drainage area of the catchment at the start of the study area is 143.4 km^2 which grows to 150.6 km^2 at the end of the study area (Figure 1). Onondaga Creek is located in a temperate climate with an annual average temperature of 9.1°C (NOAA) and 97.7 cm yr^{-1} of seasonally consistent water-equivalent precipitation (NOAA). The upper reaches of the Onondaga Creek watershed are forested, and transition to increasingly heavily urbanized land closer to the creek outlet on Onondaga Lake. The bedrock of the area is the halite and gypsum rich Vernon Shale (Kappel, 2005; Yager, 2007). The study reach has very little shading, with

riparian areas recessed 23 m from the west bank and 17 m from the east bank. Onondaga Creek bears most of the combined sewer overflow (CSO) load for the city of Syracuse (Owens, 2013) and average streamflow is around 3.66 $m^3 s^{-1}$ gaining about 0.124 $m^3 s^{-1} km^{-1}$.

The study reach receives water from one natural spring, as well as several stormwater culverts. The spring located about 248 m downstream from the start of our study reach shown in Figure 1, Site 1. A total of two constant flow stormwater culverts are located within the study area. The first is located at 672 m downstream (Site 2) and the second is located 2259 m downstream (Site 4). Discharge was obtained from the Dorwin Ave USGS gaging station (#04239000, Site 1).

3 Methods

3.1 Kinetic Measurements of Stream Temperature

In situ temperature sensors were placed at several spots along the study area to measure creek, stormwater, and spring water temperatures (Site 1, 4). These sensors consisted of two Thermochron iButtons (model DS1922L, accuracy of ±0.5°C, resolution of 0.0625°C) spaced vertically within cavities on a wooden stake. Measurements were made every ten minutes from April 9, 2017 to September 1, 2017. It is important to note that due to concrete channel of the stormwater input, temperatures at Site 4 were measured shortly downstream from the input (~2 m), meaning that the stormwater signal at this location is slightly mixed.

3.2 Flights and Thermal Imagery Collection

The thermal images for the study were collected using a Zenmuse XTR thermal camera attached to a quadcopter DJI Inspire 1™ UAV flown by a US FAA Part 107 certified pilot. The data was collected during three flights conducted on May 12, June 14, and July 19 of 2017. The UAV was flown using a pre-programmed, geolocated flight path. The same geolocated flight path was used for each flight with a flight speed of 7.6 m s^{-1} and flying altitude of 67 m above ground level. The flights occurred around 3 pm to ensure flights captured differences in temperature between the artificially channelized inputs and the stream. Pictures were taken at nadir every 21 m to ensure overlap between images. Due to the length of the study area and battery limitations, each month's TIR survey was conducted using two separate flights that covered the entire study area.

The Zenmuse XTR camera (336 x 256 pixel resolution, NEΔT <50mk at f/1.0) we used interfaced with the Inspire 1™ UAV by gimbal, observes infrared radiation with an uncooled VOx microbolometer measuring long wave infrared radiation in the 7.5 - 13.5 µm range. The measurement resolution of the camera for our flight altitude was estimated to be 0.9 m^2. For each drone flight, the air temperature, relative humidity and reflective temperature are recorded for use in correcting the TIR images, with air temperature and relative humidity measurements taken from the nearby Syracuse University weather station. Additional information on reflective temperature collection is included in Text A_1.

3.3 Post-Processing of Thermal Imagery

Thermal imagery was post-processed with FLIR Tools, an open-source software. Each thermal image was corrected for distance from the imaged object, air temperature, humidity, emissivity (ε = .98) (Buettner & Kern, 1965), and reflective temperature. Temperature and humidity were taken from the Syracuse University Weather Station, located approximately 6.4 km from the study site (https://onondaga.weatherstem.com/syracuse). Photos were georeferenced in ArcMap (ESRI) and individually masked to exclude non-stream material. After masking, photos were compiled into a complete mosaic for each month. Radiant stream temperatures were obtained from the TIR data at the spring and culvert to determine the approximate temperature of these sources as close to the installation points (Sites 1, 4) as possible. Mean radiant temperatures and variance across the channel were also extracted from continuous images approximately every 1.75 m downstream using a custom polyline shapefile (Figure 2). To estimate how radiant temperatures varied across the stream channel, we extracted several cross-sections downstream of both the spring (Site 1) and first stormwater input (Site 2). In addition, we calculated the mean and a standard deviation of stream temperature at a given downstream distance from collocated pixels extracted across the stream width from TIR imagery. As TIR imagery was prone to unrealistic swings in radiant temperature, we normalized all stream temperature photos by running each month's photos through a program in MATLAB (Mathworks). We normalized each photo to its own median temperature value. Following this correction, photos were brought back into ArcMap to extract the normalized mean and standard deviation using the collocated points and shapefile described previously.

3.4 Model Runs and Calibration

A modified version of HFLUX 3.0, an open-source, 1-D stream temperature model, was used to simulate stream temperature. We modified HFLUX by using the program's existing capability to model groundwater inputs, and expanding that capability to be able to handle changes in the volume and temperature of groundwater discharge. This allowed us to model stormwater, as groundwater and stormwater input will behave the same in a 1-D model. HFLUX is a deterministic model that creates a heat budget for a given stream to estimate the volume of groundwater discharge based on unaccounted heat in a full budget (Glose et al., 2017). We employed a similar approach to simulate the contribution of stormwater inputs, formulated as singular nodes with two parameters describing each input, stormwater discharge and temperature. As Onondaga Creek is large with clay dominated bed material, we assumed groundwater effect on stream temperature was negligible, and did not include this flux within our model formulation.

Model simulations were performed for three different periods corresponding to UAV flights. These periods include May 10 – May 15, June 12 – June 17, and July 17 – July 22, 2017. Stream temperature was simulated within HFLUX at a temporal resolution of 2 min and a spatial resolution of 1 m. For each simulation, the first 48 hours of model data were repeated for each run to serve as a warm-up period before simulating the desired five-day period in each month.

HFLUX requires a significant amount of input data. Weather data was gathered from the Syracuse University Weather Station located 6.4 km northeast of the study area. Weather station data was measured at approximately 15 minute resolution and resampled to the model timestep. Discharge into the model was gathered from a USGS gauging station within the study area (USGS 04239000). As Onondaga Creek experienced low-flow conditions and discharge remained fairly constant during modeled periods, discharge was held constant through time, with the upstream discharge for Onondaga Creek assumed to be the mean discharge for the modeled period in each month. Variable and input descriptions and sources are listed in Table A_2. Temporal model error was assed using the root mean squared error calculated between iButton observations and simulated stream temperatures at Site 4 (Figure 1) according to

$$RMSE = \sqrt{\frac{\sum_{i=1}^{n}(\hat{x}_i - x_i)^2}{n}} \quad [1]$$

where n is the number of model timesteps, $\hat{x}_i$ is the observed temperature, and x_i is the modeled stream temperature at timestep i.

While most stream temperature models compare to a discrete set of points either at the end of a reach (Westhoff et al., 2007; Leach et al., 2015) or along a stream (Glose et al., 2017), we compliment this approach by comparing model output to TIR imagery consisting of thousands of pixels distributed through space. Based on TIR data, we defined two metrics to quantify the effects of the stormwater input to assess spatial error. We sampled the 'Initial Impact' values by taking the average stream temperature across the stream channel and taking three average stream temperatures at the stormwater input source in the TIR photos for each flight. The stormwater input stream temperatures were then subtracted from the stream temperature to obtain a range of acceptable values for each month. The second metric, an 'Effect Duration', measured the downstream distance corresponding to observable stormwater input effects. The "observable effect" for each month was defined using the standard deviation of normalized radiant stream temperatures, measured as the distance at which radiant temperature standard deviations were below 0.075 °C and 0.05 °C (Figure 3). This provided a window of plausible ranges for the stormwater effects to persist. For modeled scenarios, the "Effect Duration" was defined as the point downstream at which temperature returned to within 0.1 °C of pre-stormwater stream temperature. A table of the ranges of acceptable 'Initial Impact' and 'Effect Duration' for each flight is provided in Table A_3.

3.5 Incorporating Urban Heat Fluxes

We primarily focus on one stormwater input, located 673 m downstream from the beginning of the reach (Site 2). The culvert has an unknown discharge with stream temperature recorded by UAV-based TIR. Within the model, the input was parameterized as a constant increase in stream discharge over 4 m from 670 m to 674 m downstream. To constrain the impact of stormwater on simulated stream temperature, we used discrete sampling to generate different stormwater discharge and input temperatures. Ranges for stormwater temperatures were constrained from the TIR data; for each month, we sampled from 3 °C warmer to 3 °C colder than TIR temperature data at 0.5 °C increments. Stormwater discharge was calculated as a percentage of upstream discharge in Onondaga Creek varied from 0.5% to 10% of upstream discharge. A control run where no stormwater input was added was also conducted for each month. A full list of the

modeled combinations of stormwater discharge and stormwater temperature are provided in Figures $A_2 - A_4$.

4 Results

4.1 Temperature Observations

Five months of temperature data in the creek and two inlets has revealed much about the behavior of water temperature within the stream channel and its association with storm and spring water. Both the stream and the two instrumented inlets display diurnal temperature patterns that become less prominent immediately following rain events and more prominent during low flow periods (Figure 4). Diel temperatures at the inlets varied by as little as 2°C or as much as 8°C. Main channel stream temperatures exhibited much larger temperature swings compared to the instrumented culverts. As shown in Figure 4, average stream temperatures increased from April to July as did the maximum daily range of stream temperatures. Through space, main channel stream temperatures, measured at the start and end of the study reach, experienced a very small rise in temperature from reach start to end, often less than a degree Celsius.

4.2 Radiative Temperatures

To evaluate accuracy of the TIR, we compared radiative and kinetic temperatures at each iButton installation (Figure 5), with kinetic temperatures at iButton temperature sensors extracted at the time step corresponding to each flight. TIR temperatures in May and June were cooler than iButton recorded temperatures, while values in July showed the opposite. As can be seen in Figure 5, radiative and kinetic temperatures did not approach a 1:1 relationship for any flight.

Local hydrology, namely the inputs to the stream, have a small effect on mean stream temperature that is not easily discernable from TIR extracted stream temperature data. As seen in Figure 6, the storm and spring water inputs do not result in an easily discernable drop in mean stream temperature. Mean radiant stream temperatures were also prone to thermal drift and discrete swings in temperature especially in the vicinity of bridges and other urban surfaces

(Figure 6). To reduce this variability, each radiative temperature measurement was normalized to the median temperature value from the TIR photo from which the measurement originated. The resulting data preserves the major patterns of the raw mean data, while eliminating much of the variability in radiant values.

Mapped normalized temperatures downstream of stormwater input 1 are shown for June, in Figure 7a and b. The persistence of the cold plume varied seasonally and peaked in June, the warmest of our flight dates. As shown in Figure 3, the length of this plume can be defined based on the standard deviation of pixels at creek cross-sections. The thermal effect of stormwater at each input is also prominent and definable in TIR images (Figure 7 c, d, e). The average change in temperature extracted at stormwater input 1 is included in Table S_3. This change was greatest in July, with a drop in mean stream temperature of 0.70 °C, and smallest in June, with a drop of 0.48 °C.

Cross-sectional stream temperature at and downstream from the spring and stormwater input 1, sampled from TIR data, demonstrates spatio-temporal impacts on stream temperatures (Figure 8). This analysis quantified the percentage of channel width corresponding to changes in stream temperature and variance as well as how cold the plume stays relative to the stream at various lengths downstream for each month. At stormwater input 1, the plume was 7% of stream channel width in June and 14% in May.

4.3 Model Output

Stream temperatures were dynamically simulated within a modified version of HFLUX 3.0. A total of 131 scenarios were run for each month. Scenarios were additionally resampled for June, which exhibited a much smaller target window for the 'Initial Impact' and 'Effect Duration' metrics. The simulations with the lowest RMSE each month were the control runs (no stormwater discharge), with RMSE values of 0.541 °C (May), 1.043 °C (June), and 0.625 °C (July). Of the modeled scenarios, ten simulations from May (Figure 9) and four simulations from July (Figure 10) met both spatial metric requirements. No model runs in June met both spatial metrics (Figure 11), however 45 runs did match the 'Initial Impact' metric, and one run matched the 'Effect Duration' metric. These runs that met both spatial metrics in May and July had RMSE values ranging from 0.798 °C to 0.913 °C for May and 0.864 °C to 0.895 °C for July. In June, the 45 runs matching initial impact recorded RMSE values of 1.120 °C to 1.424 °C, and the

single run matching plume duration recorded an RMSE of 1.104 °C. In all months, spatial best fits did not coincide with the combination of stormwater discharge and temperature that produced the lowest RMSE (Figure 9, 10, 11). Scenario analysis across different combinations of stormwater discharge and temperature revealed that stormwater discharge played a much larger role than stormwater temperature in influencing main channel stream temperature.

Figures 12 and 13 illustrate the tradeoffs between how combinations of stormwater discharge and temperature fit observations in space and time. We include these results for the July model runs. Through time, the run simulating no stormwater input, corresponding to the lowest RMSE value, replicates stream temperature behavior at low temperatures (night time) and the transition from low to high (beginning of the day) and high to low (afternoon to evening), but overestimates peak stream temperatures (Figure 12). Comparing this simulation to the six simulations that match both metrics for spatial behavior, we see similar patterns. Overall, differences between simulations that meet both spatial metrics versus simulations with the lowest RMSE are minimal. However, in space, this tradeoff is clear. As shown in Figure 13, a stormwater discharge and temperature of zero, removing the effect of the stormwater input, produces a distance series that does not match known behavior in the reach. In comparison, the run with the lowest RMSE that also met the 'Initial Impact requirement' for July, while matching the initial drop in stream temperature, did not adequately simulate the 'Effect Duration' simulating a much shorter duration downstream. The run with the lowest RMSE that also matched the Effect Duration metric matched best spatially as it also matched the Initial Impact metric.

We also include heat fluxes for the best spatial and temporal runs from each month in Figures A_6 – A_8. Heat gain was driven primarily by solar radiation and sensible heat flux, while heat loss was controlled by latent heat flux and longwave radiation. Comparing the 'best fit' combination of stormwater discharge and temperature, we found no discernable difference in the heat fluxes between the two runs.

5 Discussion

5.1 The Role of Stormwater in Stream Temperature Regimes

Through four months of monitoring and three UAV flights, we have explored the relationship between discrete inputs, including stormwater, to a Syracuse, NY waterway. As seen in Figure 4, temperatures in the stream are consistently warmer than those of the spring and stromwater input 2 (Site 4), with stormwater (Site 4) consistently colder than the stream temperature. Stormwater temperatures warm seasonally, but at a slower rate than the stream. Given the cold temperature of this stormwater, we observed the largest difference between stream and stormwater temperatures in July, the warmest month in 2017 for Syracuse (Figure 4). Additionally, we found that cold plumes from stormwater inputs could discernably lower mean stream temperatures while impacting a small fraction of the stream channel width (Figure 8).

Our finding that stormwater temperatures are cooler than main channel stream temperatures is contrary to findings by Van Buren et al (2000) Nelson and Palmer (2007), Somers et al. (2013), and Hathaway et al. (2017). Van Buren et al. (2000) found that runoff from parking lots in Ontario Canada is higher in temperature than upstream discharge. Nelson and Palmer (2007) demonstrated that surges of stormwater to streams in small urban watersheds in Washington DC during summer storms can increase stream temperature upwards of 7 °C. Sommers et al. (2013) found similar effects on streams draining urban catchments in Durham, NC observing increases in stream temperature up to 4 °C during summer storms. Hathaway et al. (2017) monitored urban streams in North Carolina for one and found similar results with change in stream temperature as a result of storm runoff to those by Somers et al. (2013) with an average of 2-3 °C change in stream temperature as a result of runoff from summer storms. We saw no indication that stream, or even stormwater temperature increased as a result of precipitation events (see Figure A_5). As compared to previous work in North Carolina (Somers et al., 2013, Hathaway et al. 2017), Syracuse has a much colder climate and fewer warm, convective summer storms. We also note that the Onondaga Creek watershed is much less urbanized and much larger than most of those studied by Nelson and Palmer (2007), Somers et al. (2013), and Hathaway et al. (2017) with 9% urbanization over the entire watershed, and 45% urbanization in the immediate surroundings of our study area. As our work is primarily examining a few sites along a single stream, our findings may not be applicable for all systems in Syracuse, but do suggest stormwater may not be a source of thermal pollution in Syracuse, NY, with potential implications for other northeastern cities. More work characterizing the behavior of stormwater along rural to urban gradients is needed to better inform this relationship.

5.2 Challenges of using UAV-based TIR Imagery

Through three UAV-based TIR surveys of our study area and comparing the TIR recorded temperatures to in-stream temperature sensors, we found that TIR imagery is unreliable for absolute temperature values (Figure 5). This is due to perceived temperatures, which fluctuated significantly though space and time (Figure 6), as well as perceived radiative temperatures fluctuating between being warmer and colder than the corresponding kinetic temperature observations (Figure 5). Additionally, within each month, while linear, the relationship between radiative and kinetic temperature observations is not 1:1 resulting in a changing amount of error between the two with space and time (Figure 5). This is contrary to results from Handcock et al. (2006) that compared aerial (airplane and helicopter) and satellite-based TIR and found that after radiometric corrections had been applied, images with more than 3 pixels across the targeted stream, while overestimating stream temperature, had approximately a 1:1 relationship between radiative and kinetic temperature observations. The inaccuracy of our TIR imagery may be attributed to new variables present for UAV-based TIR as opposed to airplane, helicopter or satellite-based TIR, including variable cloud cover and weather conditions, variable reflective temperature, the need for multiple images to survey the entire study area, and the use of an uncooled system as opposed to the cooled systems used in Handcock et al. (2006). Currently, UAV payload limitations prevent use of higher resolution TIR cameras or cooled system TIR cameras (Dugdale, 2016). Cooled systems are generally more accurate and have higher resolution than uncooled systems at the same altitude and often operate in the short and medium wave bands of TIR, and can only be deployed via airplane, helicopter and satellite. As technology continues to advance and UAV capabilities and sizes of sensor payloads continue to improve, deploying higher resolution or cooled TIR systems via UAV may be possible.

While UAV-based TIR has been used to study stream temperature in previous studies (Jensen et al., 2012; Nishar, 2016; Lee et al., 2016), no studies to date have discussed the issues we have encountered with TIR imagery. This may be due to the type of microbolometer used and sensitivity (NEΔT) of the cameras in the aforementioned studies. Jensen et al. (2012) used a camera from Infrared Cameras Inc. While the camera model is not listed, ICI cameras that fit the description in Jensen (2012) use a uncooled VOx microbolometer, similar to the one used in our

Zenmuse XTR, and have a higher sensitivity than our camera (20 mK at 30 °C). Nishar (2016) used the FLIR Tau 320 which uses the same sensor and has the same NEΔT as the Zenmuse XTR in this study. Lee et al. (2016) used a FLIR T450sc. The T450sc also uses an uncooled VOx microbolometer, but has a more sensitive NEΔT (<30mK). We do note that other studies do typically conduct radiometric corrections on UAV-based TIR imagery, however, the issues we encounter are present after such corrections have been conducted. Increased camera sensitivity, more stable atmospheric variables, fewer photos used, shorter sampling times, and morfe rural study areas may have influenced the presence, or lack thereof, of these post-correction temperature variations in Jensen et al. (2012), Nishar (2016), and Lee et al. (2016). We note that in particular, extreme shifts in observed temperatures from TIR corresponding to warmer temperatures were collocated with the many bridges,and other urban surfaces along the creek. While these locations were excluded from the images, they still produced warmer radiant temperature measurements due to thermal contamination. Additional corrections beyond radiometric corrections for emissivity and atmospheric variables are typically performed by fitting a relationship between radiant and kinetic temperatures (Figure 5) and correcting radiant temperatures based on this relationship (e.g., Jensen et al., 2012). As can be seen in Figure 5, we found this relationship to vary for each of our flights, suggesting that varying weather conditions likely played a role, given flights were conducted at the same time of day and the sites did not change at all from month to month.

5.3 Merits of Using UAV-based TIR Imagery

Data collection via UAV-based TIR surmounts many of the issues encountered with airborne TIR and satellite-based TIR by taking photos at nadir and eliminating the need to correct for atmospheric effects on radiant temperatures. UAV data collection is also a much cheaper alternative to airborne TIR (Dugdale, 2016; Lee et al., 2016). Low flight altitudes from UAV-based images allowed us to put dozens of pixels on target across the stream channel as opposed to as few as one pixel on target in studies using aerial or satellite-based TIR (Handcock et al. 2006; Handcock et al. 2012). This facilitates the creation of high resolution 2D temperature profiles. Within this study, TIR imagery was able to demonstrate and quantify the spatio-temporal impacts of spring water and stormwater (Site 2) on two-dimensional mean stream temperature. Although TIR may be unreliable for collecting absolute temperature, even when

normalized to the photo from which the data originated (Figure 6), we find TIR is reliable for qualitative evaluations of the impacts, and duration of those impacts, from discrete inputs (Figure 7). It is important to note that since most objects are opaque in TIR, meaning that TIR cameras cannot image temperatures deeper than those on surface of most materials. Therefore, TIR data only provides skin temperatures of imaged objects. Thus, given that our inputs are colder than the stream, our TIR imagery may understate the prominence of the cold plume generated by stormwater inputs in the creek water column.

5.3 Stream Temperature Modeling

One dimensional stream temperature modeling has been extensively studied and used to simulate effects of land use change on urban streams (LeBlanc et al., 1996), human-caused thermal degradation (Poole and Berman, 2001), stream temperature with high resolution distributed temperature sensing (Westhoff et al., 2007), climate change effects on surface water quality (Whitehead et al., 2009), the impact of urban environments on rivers and small watersheds (Hathaway and Sharples 2012; Sun et al. 2015), and to identify point source and diffuse sources of groundwater using a heat budget (Glose et al., 2017). However, few studies have simulated impacts of stormwater inputs on stream temperature using deterministic models (Van Buren et al., 1999, He and He, 2008; Thompson et al., 2008; Sabouri et al., 2016). While TIR has been used to model other hydrologic processes (Mallick et al. 2018), no examples of deterministic stream temperature modeling using TIR data yet exist in the literature. Our study demonstrates that TIR imagery can be used, albeit indirectly, to constrain hydrologic processes within a model. Work performed in this study is similar to an approach described in Glose et al. (2013), where HFLUX was calibrated to the location and magnitude of temperature change corresponding to a natural spring discharge measured with a distributed temperature sensing (DTS) cable. Indeed, DTS represents another novel data source that can help constrain spatially distributed stream temperature responses within a model framework.

Modeled behavior conforms to in situ and TIR based observations: stormwater fluxes manifest as an abrupt cooling in stream temperature followed by gradual downstream warming to pre-input temperatures. Across all months we found that stormwater discharge has a much larger effect on mean stream temperature than the temperature of the stormwater. Our results show that stormwater discharge, in order to match the initial impact and duration of cold plumes

observed in our study area measured from the TIR data, can be as little as 2.5% or as much as 10% of the original stream discharge (Figure 9, 10, 11). While several runs for May and July met both spatial metrics (Figure 9, 10), no June model runs matched both the 'Effect Duration' metric and 'Initial Impact' metric, indicating that June stormwater simulations were in disagreement with thermal plume length. In particular, simulations that replicated the 'Initial Impact' temperature produced plumes that persisted for a distance that greatly exceeded estimates from TIR imagery while the run that matched plume duration had an initial impact much smaller that was allowed for by June's 'Initial Impact' window (Figure 3). June was a particularly unusual month, with the largest difference between stormwater and creek temperatures, a total of 12.9 degrees. Given these differences, it is very likely that the TIR data underestimated the plume length, as TIR is only sensing skin temperatures thereby potentially missing the colder, denser water of the stormwater plume that is likely present lower in the creek water column. Thus, colder stormwater may be persisting for a greater distance than can be imaged by TIR, our model results reflect this showing much larger durations than predicted by runs that meet the 'Initial Impact' metric (Figure 11). June TIR data also had the most pronounced impacts from reflectivity (Figure 6), which adds uncertainty to our extraction of an 'Effect Duration' distance metric.

Overall, constraining the stormwater impact and duration led to improved model accuracy through space (Figure 12), however, resulted in less accuracy through time (Figure 13). There are other examples within the modeling literature that show disagreement between parameter combinations that match error metrics versus different metrics that represent behavior of a given variable of interest (Seibert and McDonnell, 2002; Kirchner, 2006). Our work shows similar outcomes for stream temperature modeling, as well as the value of adding field observations to better constrain spatio-temporal patterns of response.

6 Conclusion

Our study has revealed that stormwater in a local Syracuse creek is colder than mean stream temperature during May, June, and July. This may be for several reasons including climate and dominant sources of precipitation, as well as a larger catchment size and reduced urbanization when compared to previous studies on the effects of stormwater. In particular, TIR imagery allowed us to create and effectively continuous sampling of stream temperature in two

dimensions. This enabled investigation of stream temperature heterogeneities both across and down the stream channel. TIR also shows us that those heterogeneities, when caused by a stormwater input, can persist for hundreds of meters downstream from the source. As we demonstrate, UAV-based TIR collected from a particular sensor employed in this study, the Zenmuse XTR thermal camera, was unreliable for absolute temperature readings. However, imagery was reliable for qualitatively characterizing heterogeneities in stream temperature, including the start, relative magnitude, and extent of cold plumes within Onondaga Creek.

Stream temperature models have been proven to reliably simulate stream temperature in a variety of conditions and environments (LeBlanc et al., 1996; Poole and Berman, 2001; Whitehead et al., 2009; Glose et al. 2017), but few have modeled discrete changes in stream temperature from urban point sources (Van Buren et al., 1999, He and He, 2008; Thompson et al., 2008; Sabouri et al., 2016). To simulate the impacts of stormwater on local creek temperatures, our study demonstrates a novel approach for using TIR imagery to constrain deterministic stream temperature simulations. We drew from two different sources of information provided by 2D TIR imagery to assess model realism associated with different combinations of stormwater discharge and temperature. Modeling revealed discrepancies between the runs that best fit temporally (RMSE) and those the match best spatially ('Initial Impact' and 'Effect Duration') with observed data. While differences in RMSE were minor between our best temporal and spatial fits, the differences between best temporal and spatial fits were striking, with the best temporal fit in each month being the model run that made no attempt to model stormwater input. This suggests a need to calibrate stream temperature models in multiple dimensions as calibrating in a single dimension may not be able to adequately simulate the hydrologic processes attempting to be modeled.

Thermal infrared radiation collected by UAV has been proved useful for reach-scale and smaller studies (Jensen et al., 2012; Dugdale, 2016; Nishar et al., 2016) to reveal and characterize heterogeneity in stream temperature across and downstream. Our work demonstrates that UAV-based TIR may be useful in urban environments for revealing complex patterns of interaction between discrete stormwater sources and main channel stream temperatures. Given literature emphasis on mapping the impacts of urban stormwater on stream thermal regimes, UAV-based TIR is likely a useful approach for fingerprinting urban water

sources. Beyond urban systems, our work contributes to the growing body of literature assessing simulations of hydrologic processes using novel techniques. UAV imagery is yet another approach that can be used to improve our understanding beyond its ability to easily, and cost-effectively observed remote, or hard to reach sites, UAV imagery, in any spectral band, but especially in TIR, offers the ability to sample 2D data in high resolution. High resolution field observations of spatial and temporal patters will be critical to future work in hydrologic modeling (e.g., Kirchner et al., 2006). As this study shows, attempts to model physical processes must be calibrated in multiple dimensions or risk over-simplifying important processes and interactions within the study area.

7 Figures

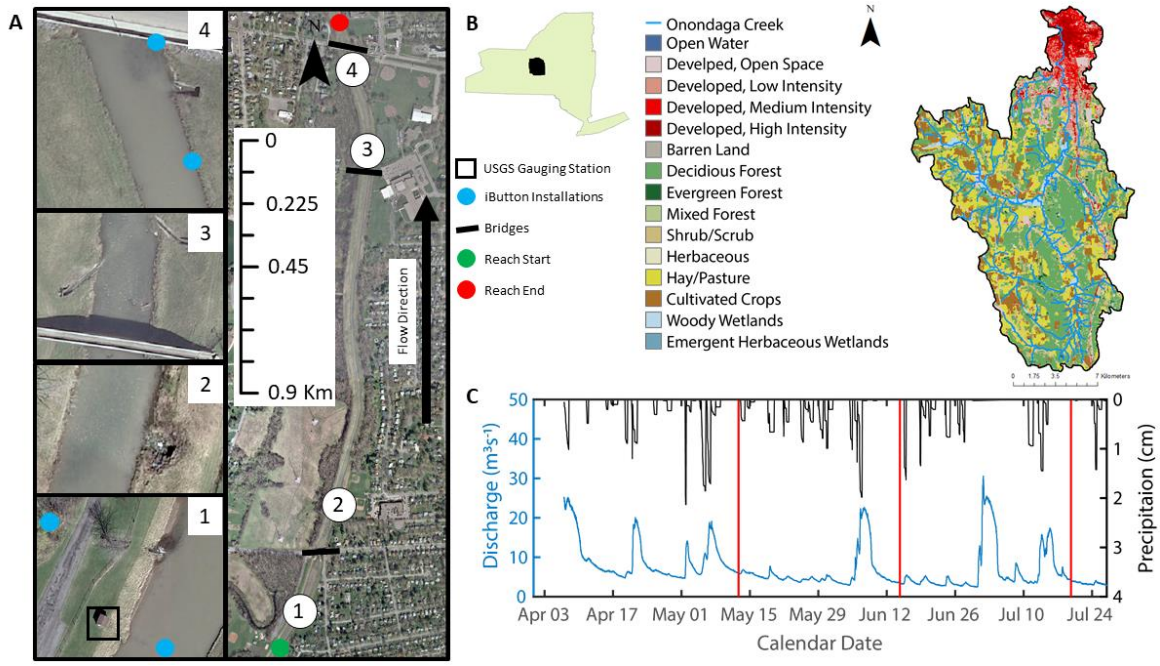

***Figure 1**: A (a) high resolution view of the study site that is located within (b) Onondaga County and the Onondaga Creek watershed. The study site consists of a 2.25km stretch of Onondaga Creek; the model start and end points are shown by the green and red dots, respectively. Bridges are identified with black dots. Site 1: The Dorwin Ave USGS stream gauging station (black box), natural spring (245.96 m), and the Spring and Dorwin Ave ibutton installations (blue dots). Site 2: Stormwater input 1 (670.20 m). Site 3: The pedestrian bridge and two non-constant stormwater inputs. Site 4: Stormwater input 2 (2258.76 m) and the Rt 173 and Stormwater input 2 iButton installations (blue dots). Land use (b) for Onondaga Creek transitions from forested to heavily urbanized within the study area. Timeseries of (c) precipitation and discharge are shown for the length of the study, with red lines indicating flight dates.*

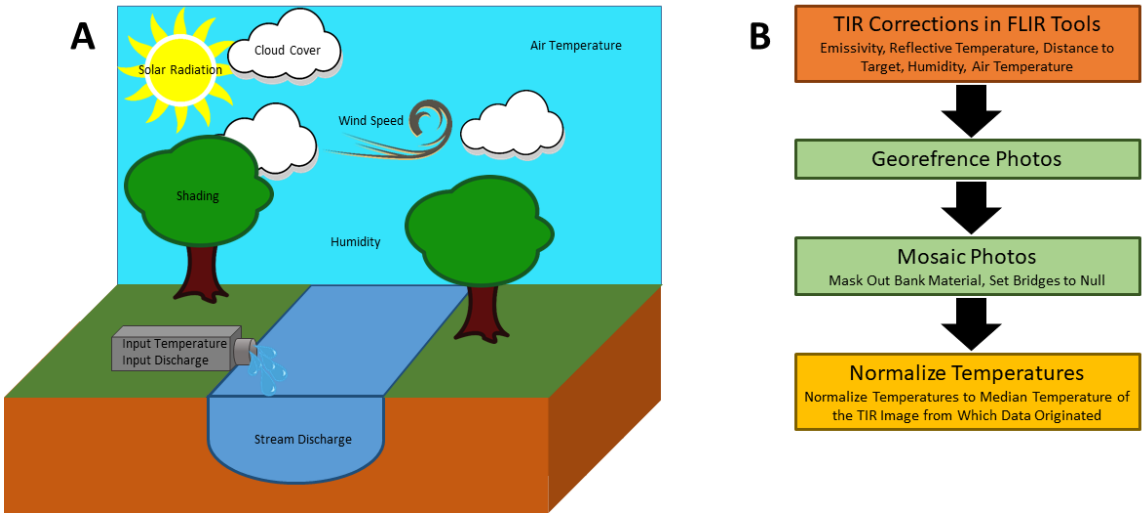

***Figure 2**: The (a) weather variables and hydrologic processes that affect heat fluxes to and from the stream, alongside (b) a work flow diagram to illustrate the processes necessary to prepare TIR data for use in the model.*

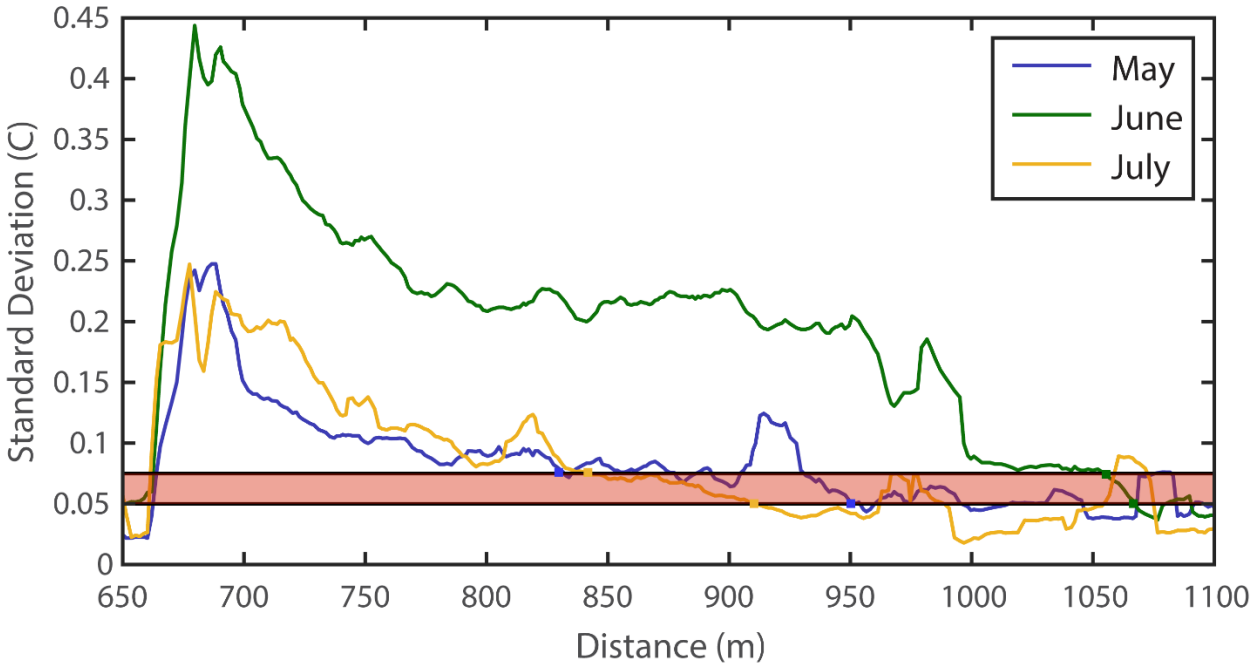

***Figure 3**: The standard deviation of stream temperature, in degrees Celsius, across the channel as measured by the TIR data. Data is shown for May (blue), June (green), and July (yellow). The red bar represents the upper and lower bounds (0.075 and 0.05 °C) for when stormwater input 1 ceases to impact average stream temperature.*

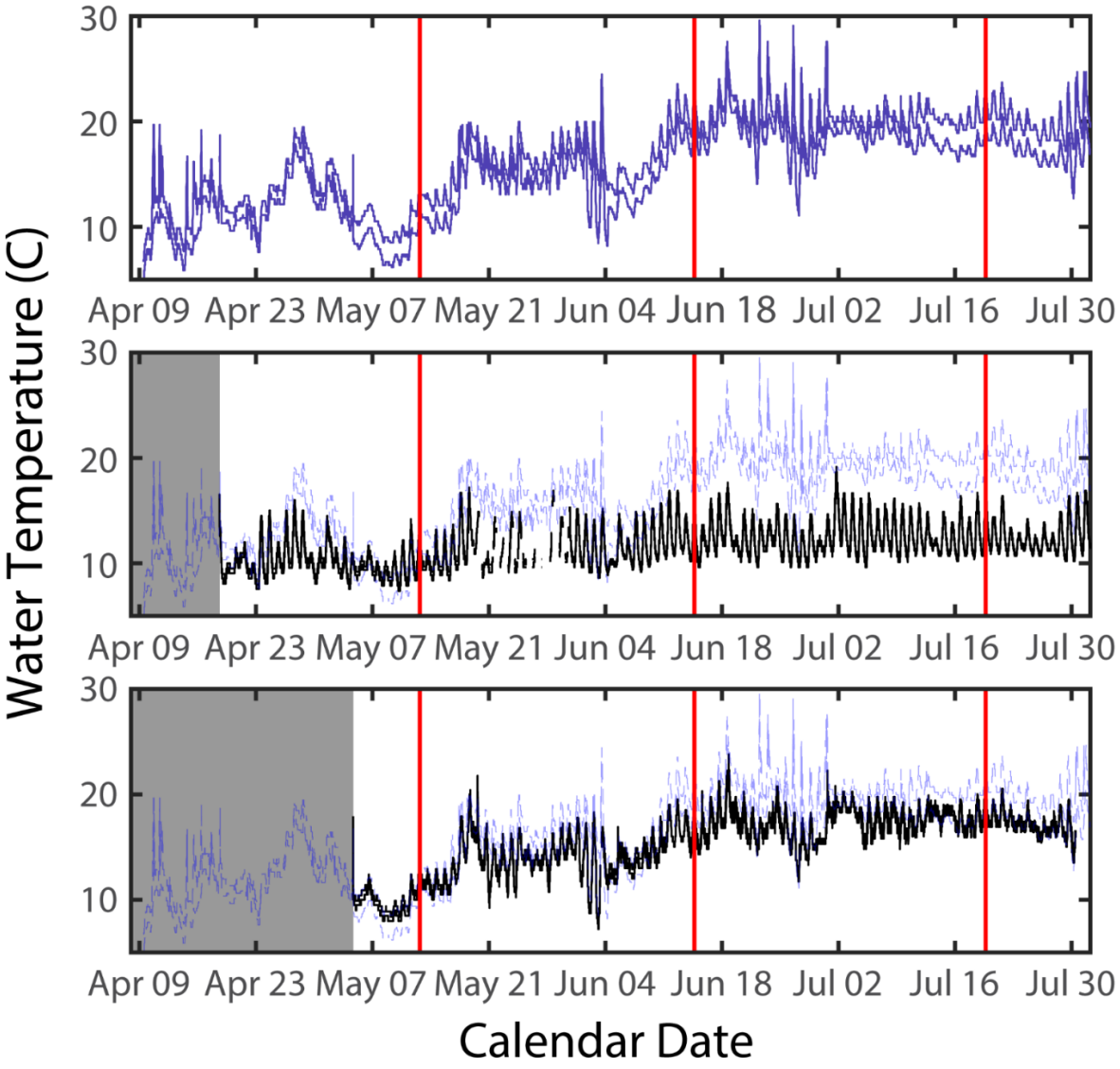

Figure 4: *Stream temperatures measured by the iButton installations in the stream (top), spring (middle), and stormwater input 2 (bottom). Red lines indicate flight dates. Main channel stream temperatures are shown in light blue in the middle and bottom panels, to enable comparison to spring and stormwater temperatures. Grey areas represent periods of time where spring and stormwater temperatures were not monitored.*

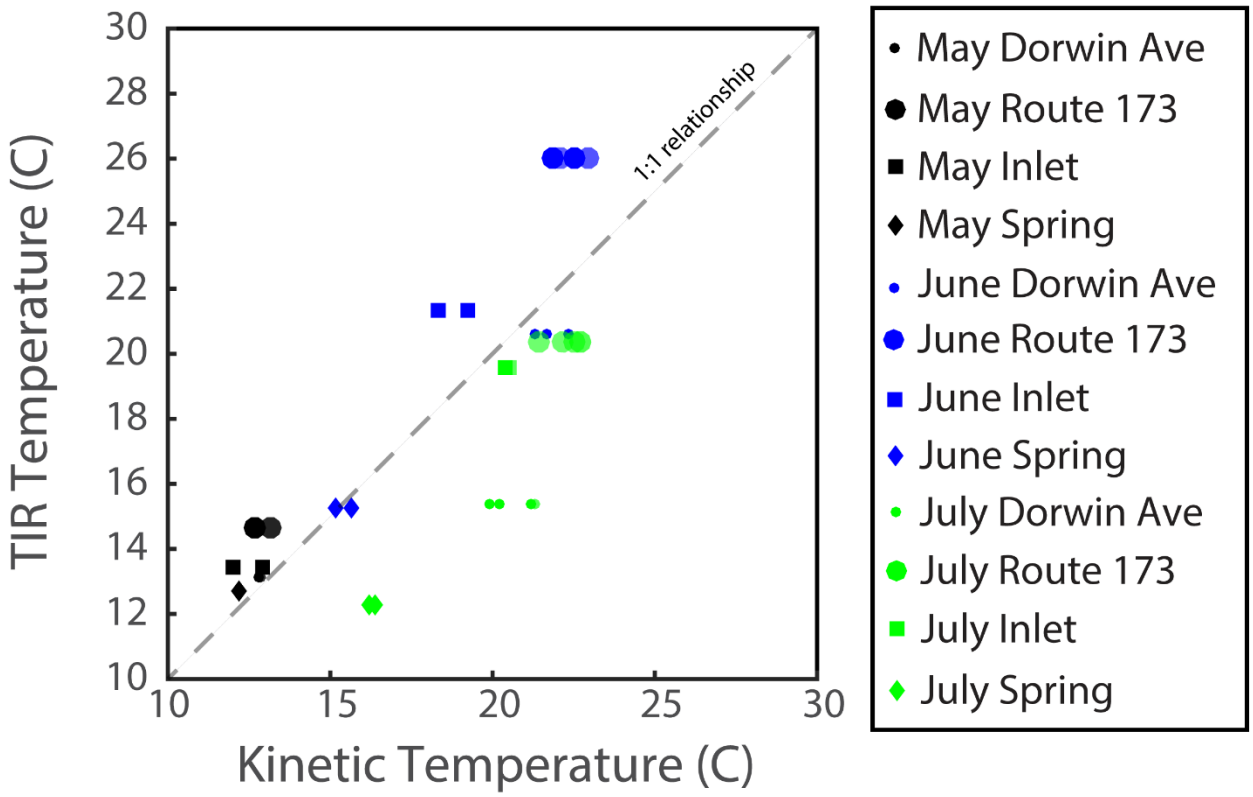

***Figure 5**: Kinetic (iButton) temperatures versus temperatures measured by TIR (radiant temperatures). Symbol shape corresponds to different measurement sites and color corresponds to the three flight dates.*

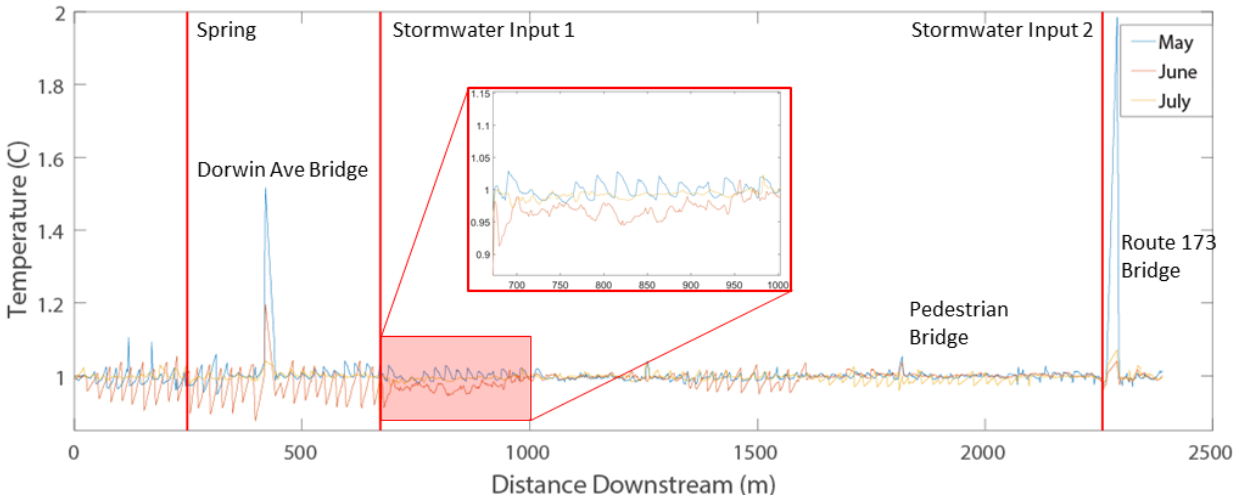

***Figure 6**: Distance series of the average temperatures across the stream channel measured by TIR for each of the three flights. Red lines indicate constant inputs to the stream. The smaller graph is a magnification of the effect of stormwater input 1 on average stream temperature*

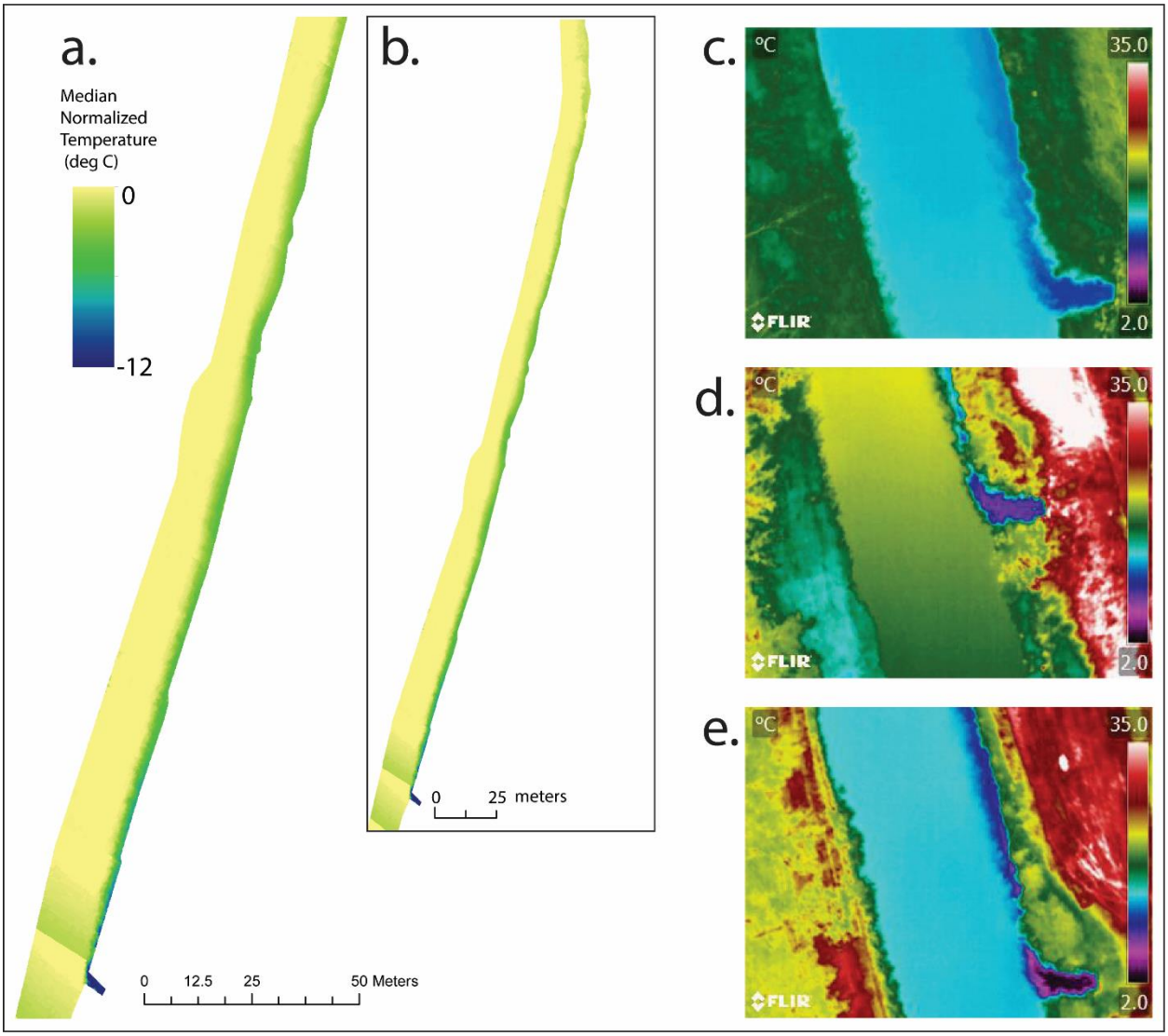

***Figure 7**: Shows (a) stitched images of normalized TIR of stormwater input 1 (Site 2) for June with (b) a zoomed-out image of the same input. Reflectivity issues are apparent at the bottom left corner of (a) and (b). TIR images of stormwater input 1 for May, June, and July (c), (d), and (e). Reflectivity issues are apparent in the creek in (d).*

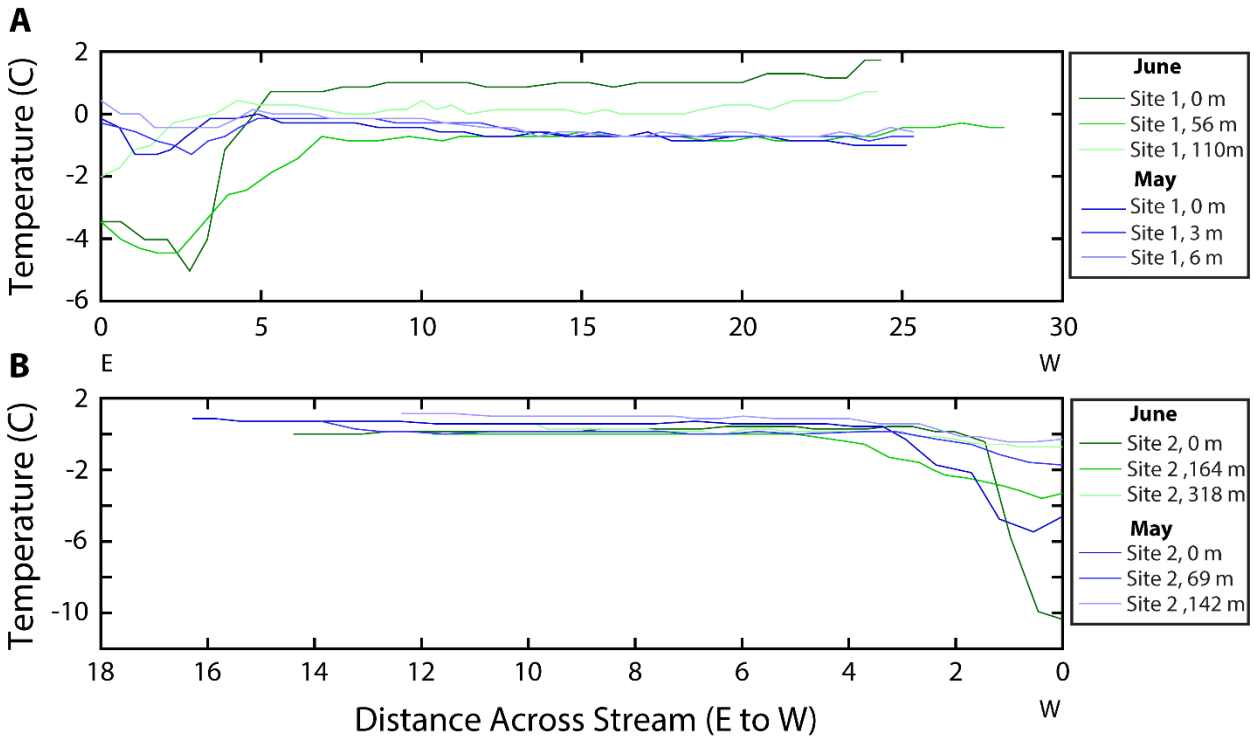

***Figure 8**: Shows (a) cross sections of stream temperature at the start, middle, and end of the cold plume generated by the spring in June and May. Also shown are (b) cross sections of stream temperature at the start, middle, and end of the cold plume generated by stormwater input 1 in June and May. Moving left to right on both graphs is East to West in the stream*

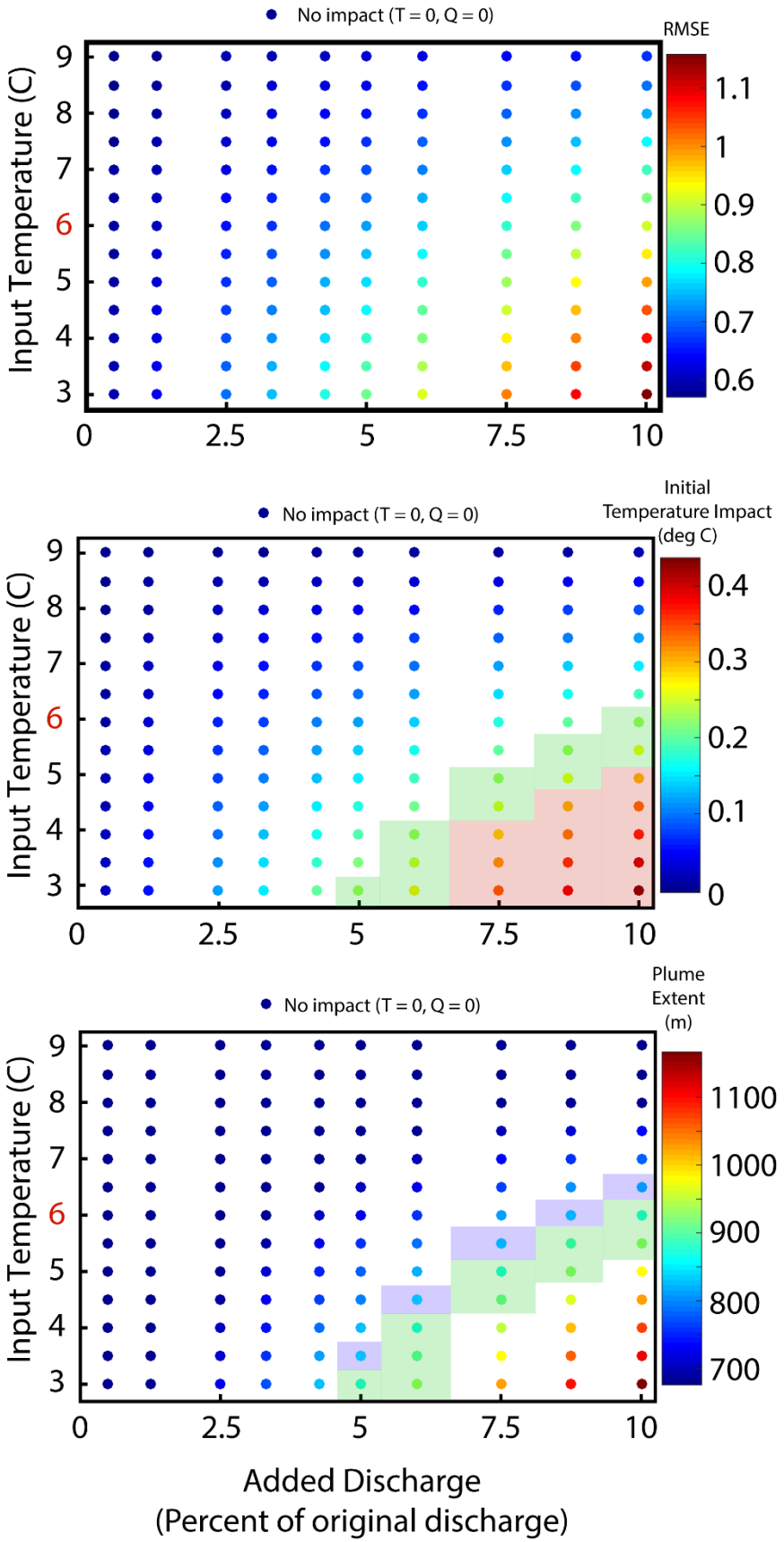

***Figure 9**: Shows the RMSE (°C) (top), Initial Impact (°C) (middle), and Effect Duration (m) (bottom) for May model scenarios. Combinations of stormwater temperature and discharge that match Initial Impact metrics are in the red shaded region, those that match the Effect Duration metric are shown in the blue shaded region. Combinations that match both are shaded in green. The red number on the y-axis indicates the temperature of the stormwater input as measured by TIR.*

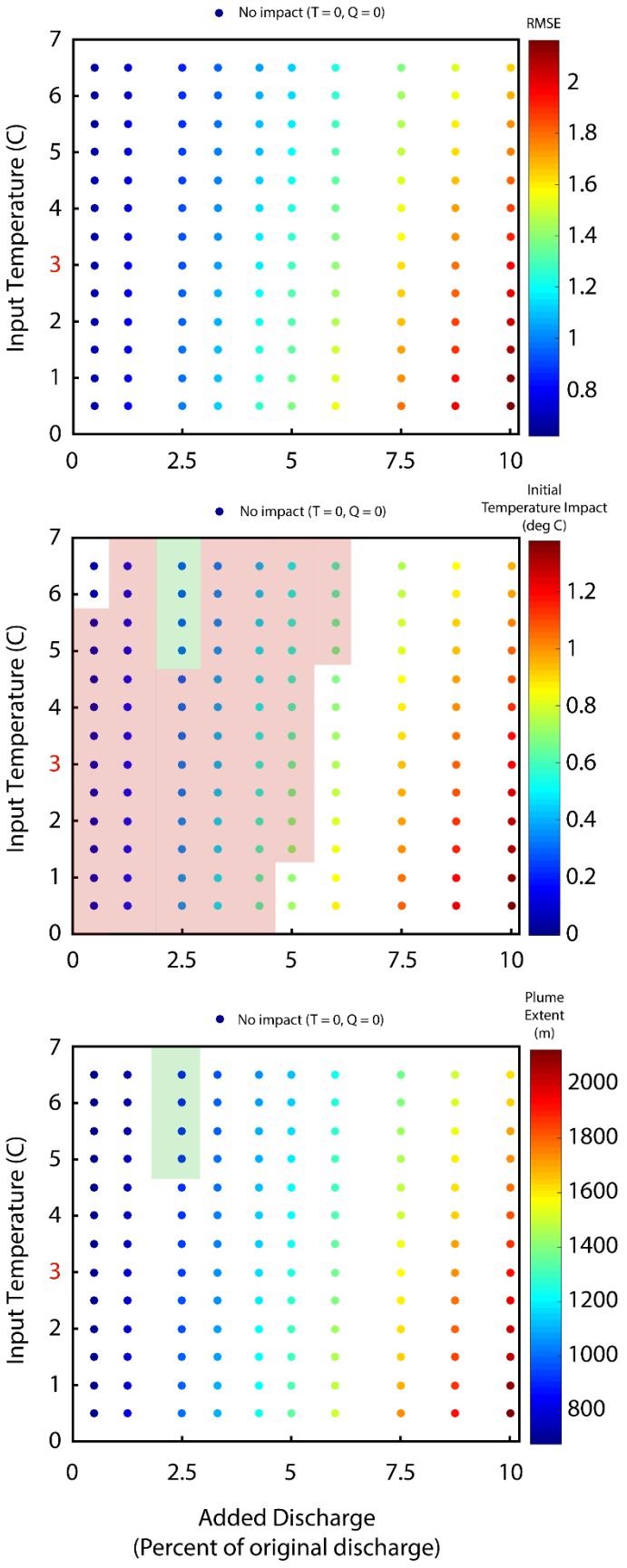

***Figure 10**: Shows the RMSE (°C) (top), Initial Impact (°C) (middle), and Effect Duration (m) (bottom) for July model scenarios. Combinations of stormwater temperature and discharge that match Initial Impact metrics are in the red shaded region, those that match the Effect Duration metric are shown in the blue shaded region. Combinations that match both are shaded in green. The red number on the y-axis indicates the temperature of the stormwater input as measured by TIR.*

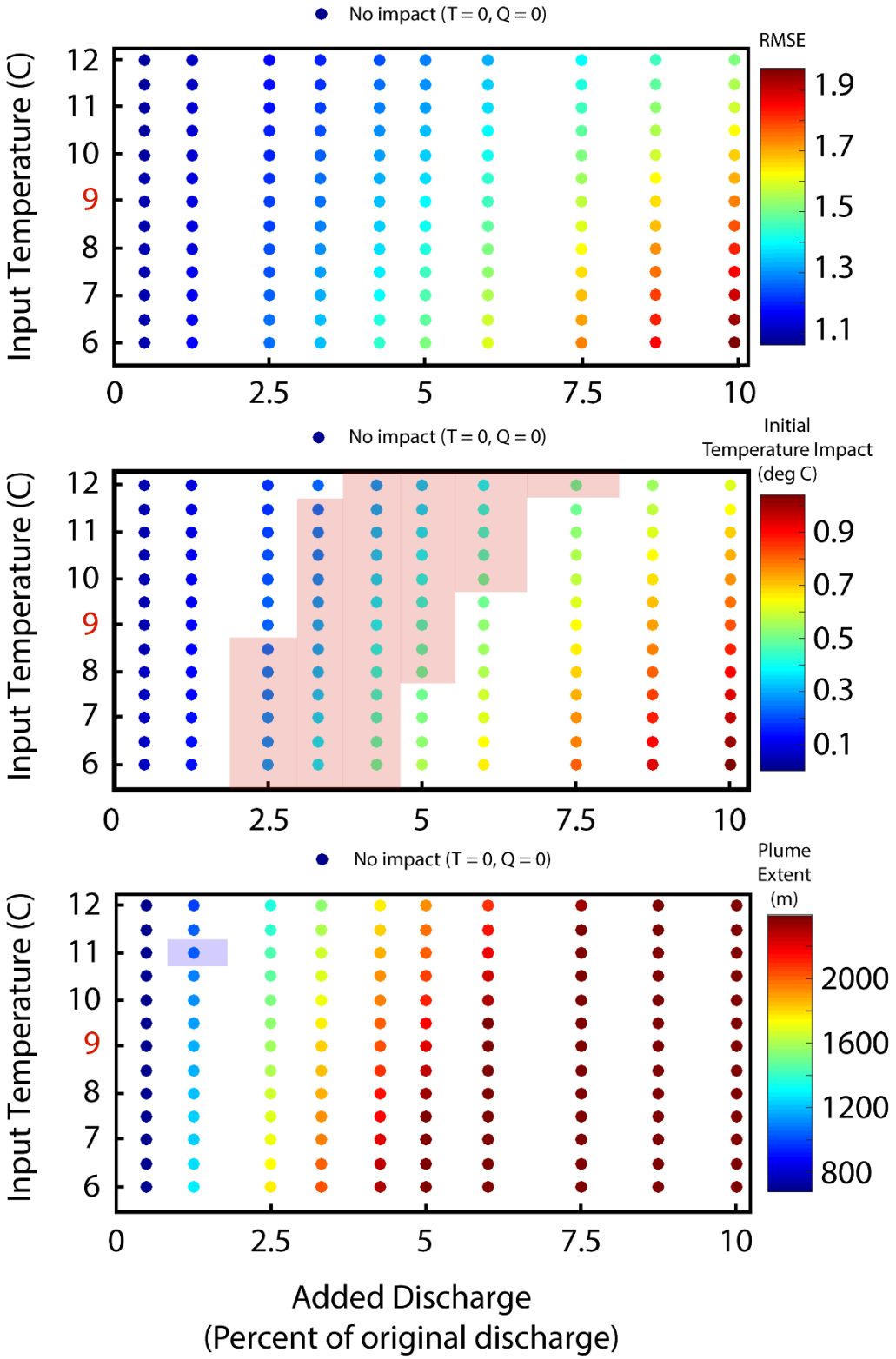

***Figure 11**: Shows the RMSE (°C) (top), Initial Impact (°C) (middle), and Effect Duration (m) (bottom) for Jun3 model scenarios. Combinations of stormwater temperature and discharge that match Initial Impact metrics are in the red shaded region. No model runs for June matched both spatial metrics. The red number on the y-axis indicates the temperature of the stormwater input as measured by TIR.*

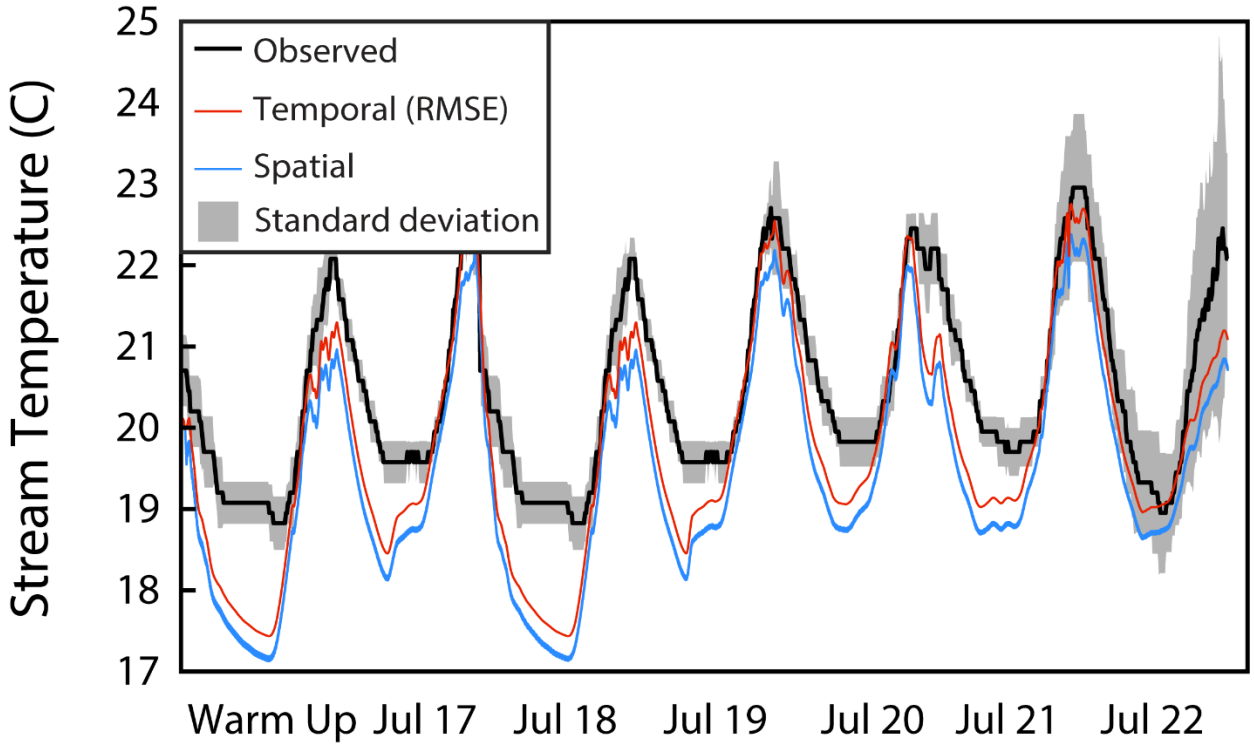

***Figure 12**: The average observed stream temperature timeseries (black) plotted alongside the six combinations of stormwater discharge and temperature that conformed to spatial metrics (red) and the simulation with the lowest RMSE (blue) for July modeling. The grey area represents the standard deviation of the iButton data.*

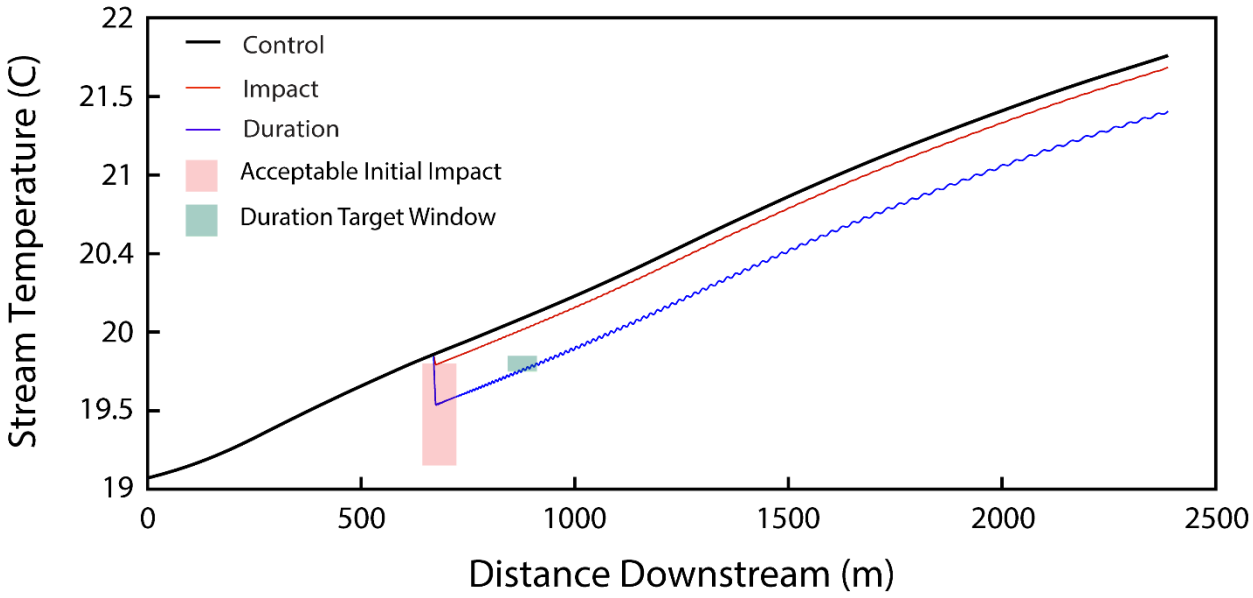

***Figure 13**: Distance series of the simulations with the best match for RMSE (black), Initial Impact (red) and Effect Duration (blue) for July simulations. 'Initial Impact' and 'Effect Duration' series correspond to a single simulation with the lowest RMSE that meets each of these spatial metrics. The red, and blue shaded areas represent the appropriate windows for Initial Impact and Effect Duration target window respectively. The target window is defined as the point at which stream temperature returns to within 0.1 °C of pre-stormwater stream temperature and falls within the corresponding month's acceptable distance range.*

8 Appendix

Text A_1:

Reflective temperature is mentioned in the manuscript as an important variable in radiometric corrections for TIR data. We provide the procedures we sued to sample reflective temperature below and an example of sampled reflective temperature in Figure S_1. Table S_1 in this section also gives the different atmospheric conditions and other variables relevant to radiometric corrections for each of the three TIR surveys.

Reflective Temperature Sampling Procedures:

1. Obtain a large sheet of cardboard, at least 1 m^2
2. Obtain enough tin foil to completely cover one side of the cardboard sheet
3. Thoroughly Crumple the tin foil
4. Carefully un-crumple the tin foil
5. Use the stretched-out crumpled tin foil to cover your cardboard sheet, and fasted the tin foil in place. This will result in light from almost every angle being reflected from a low emissivity surface to the TIR camera when sampling reflective temperature.
6. When conducting TIR surveys, begin each survey with a photo of the foil-covered cardboard sheet. **Emissivity should be set to 1.0 and the distance to target on the TIR camera should be set to 0 for this photo**.
7. Average the temperatures recorded across the cardboard sheet (we did this in FLIR Tools using the Box tool). This average temperature is your reflective temperature (Figure S1.1)

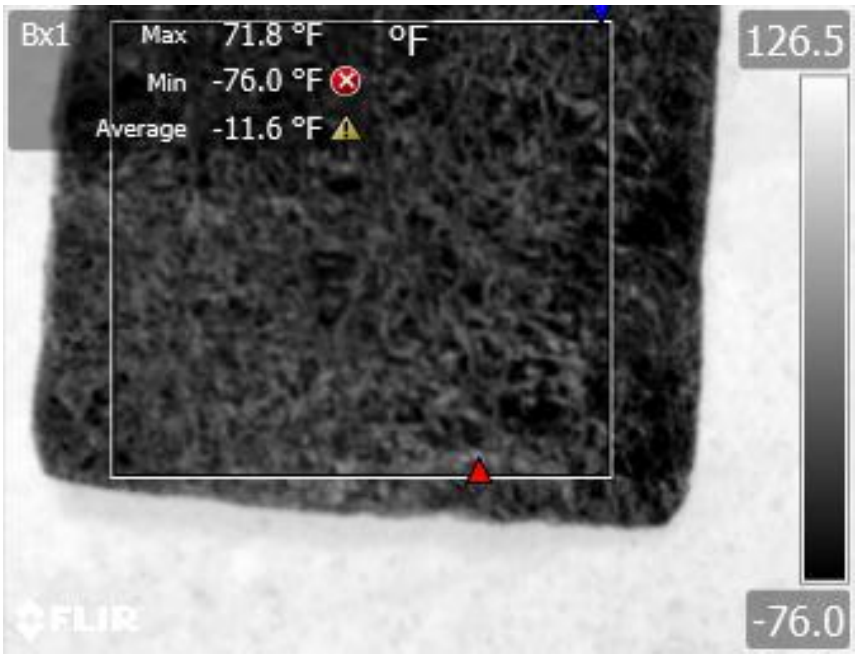

Figure A3: Shows the reflective temperature measurement for our June TIR Survey sampled using the Box tool in FLIR Tools. Temperature readings are so extreme due to the foil reflecting the sky, which always reads extremely negative temperatures when imaged in TIR.

Table A1: Gives the data used for radiometric corrections in FLIR Tools for each of the three TIR surveys.

Month	Emissivity	Refl. Temp. (°C)	Distance (m)	Atm. Temp (°C)	Humidity (%)
May	0.98	12.1	60.96	18.9	44
June	0.98	-25	60.96	25	29
July	0.98	12	60.96	29.4	50

Text A_2

The HFLUX model requires a large amount of input data. That data, its variable name, description, and source is listed below in Table S_1. The minimum and maximum values of 'Effect Duration' and 'Initial Impact' for each month are given in Table S_2.

Table A2: A summary of the model input data, their description, and source. Variable names and descriptions were modified from Glose et al. (2017).

Variable	Description	Source
time_mod	Model timesteps (min)	Set by user
dist_mod	Model spatial steps (m)	Set by user
temp_xo_data	Temperatures (°C) through time (min) the first spatial node (x = 0)	iButtons
temp_to_data	Temperatures (°C) with distance (m) at the first timestep (t = 0)	iButtons
dim_data	Stream dimensions: cross-sectional area (m^2), width (m), and depth (m) at specified locations along the modeled reach (m)	measured in field
dis_data	Total stream discharge rates (m^3/s) at given distances.	USGS Dorwin Ave station
time_dis	The timesteps of discharge rates given in dis_data (min)	USGS Dorwin Ave station
T_L	Stormwater temperatures (°C) at given distances (m) and times (min)	Monte Carlo Experiment
met_data	Meteorological data: Solar radiation (W/m^2), air temperature (°C), relative humidity (%), and wind speed (m/s) with date and time of observation	Syracuse University Weather Station (Life Sciences Center)
bed_data1	Distances (m) and depths (m) of streambed observations	based on results of a Monte Carlo experiment
bed_data2	Streambed temperatures (°C) through time (min) at bed_data1 locales	based on results of a Monte Carlo experiment
sed_type	streambed sediment type (clay, silt, sand, or gravel) at bed_data1 locales	measured in field
shade_data	Shading [0 (no shade)-1 (full shade)] and view to sky [0 (no view)-1 (full view)] at given distances (m) along the modeled reach	measured in field
cloud_data	Cloud cover [0(none)-1 (full)] through time (min)	measured in field
site_info	Site location information: latitude, longitude, time zone (5-8 for continental US), and elevation above sea level	Syracuse University Weather Station (Life Sciences Center)

Table A3: Shows the minimum and maximum 'Effect Duration' in meters downstream from the reach start as well as the upper and lower boundaries for the 'Initial Impact' metric in ° C.

Month	Min Effect Duration	Max Effect Duration	Initial Impact High	Initial Impact Low
May	833	955	0.487	0.224
June	1056	1068	0.479	0.227
July	843	911	0.701	0.052

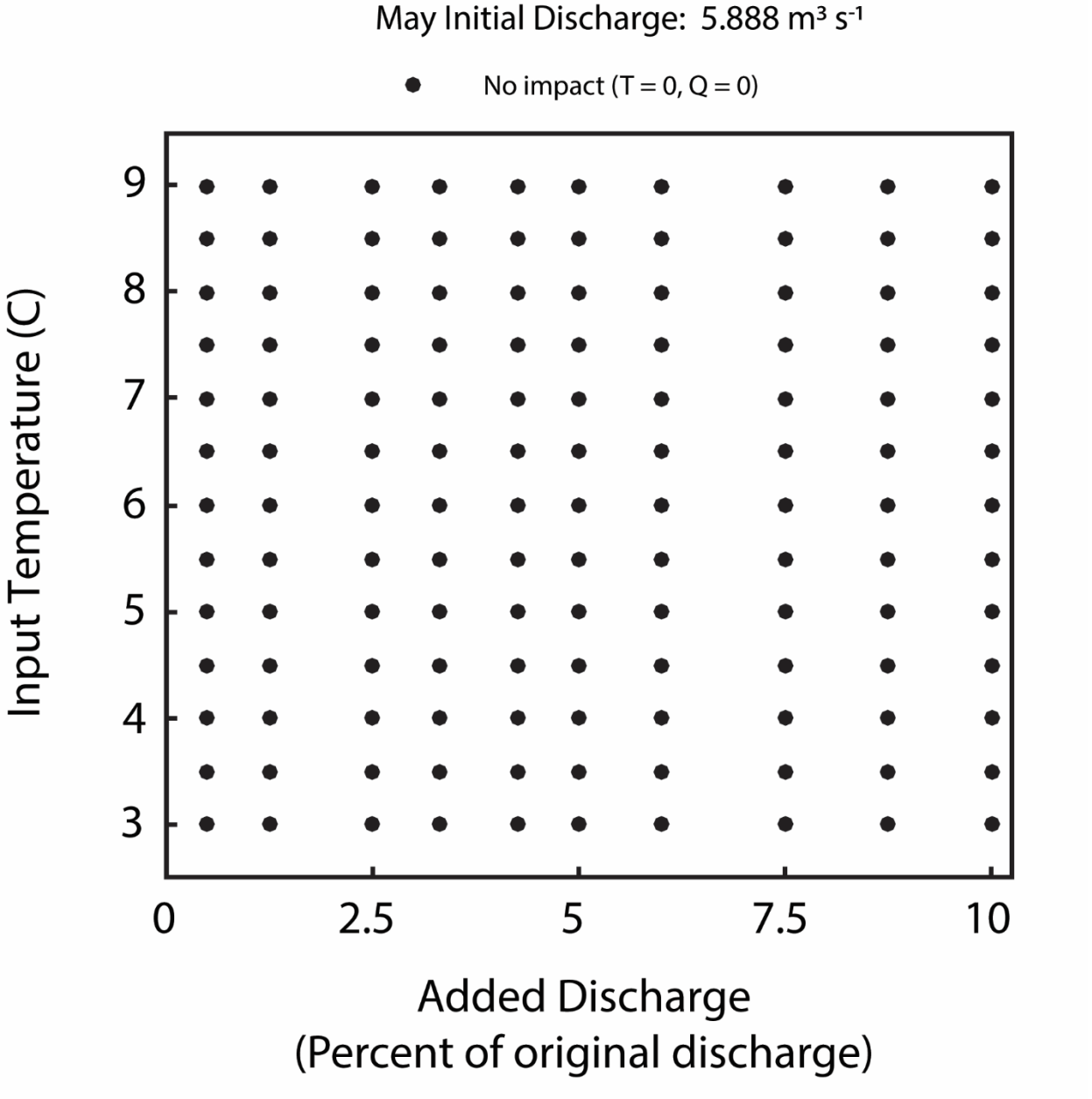

Figure A$_2$: Shows the different combinations of stormwater temperature (°C) and discharge (% of original discharge) for May. Each point represents one unique combination including a no impact run of no stormwater input. Original discharge is given above the figure.

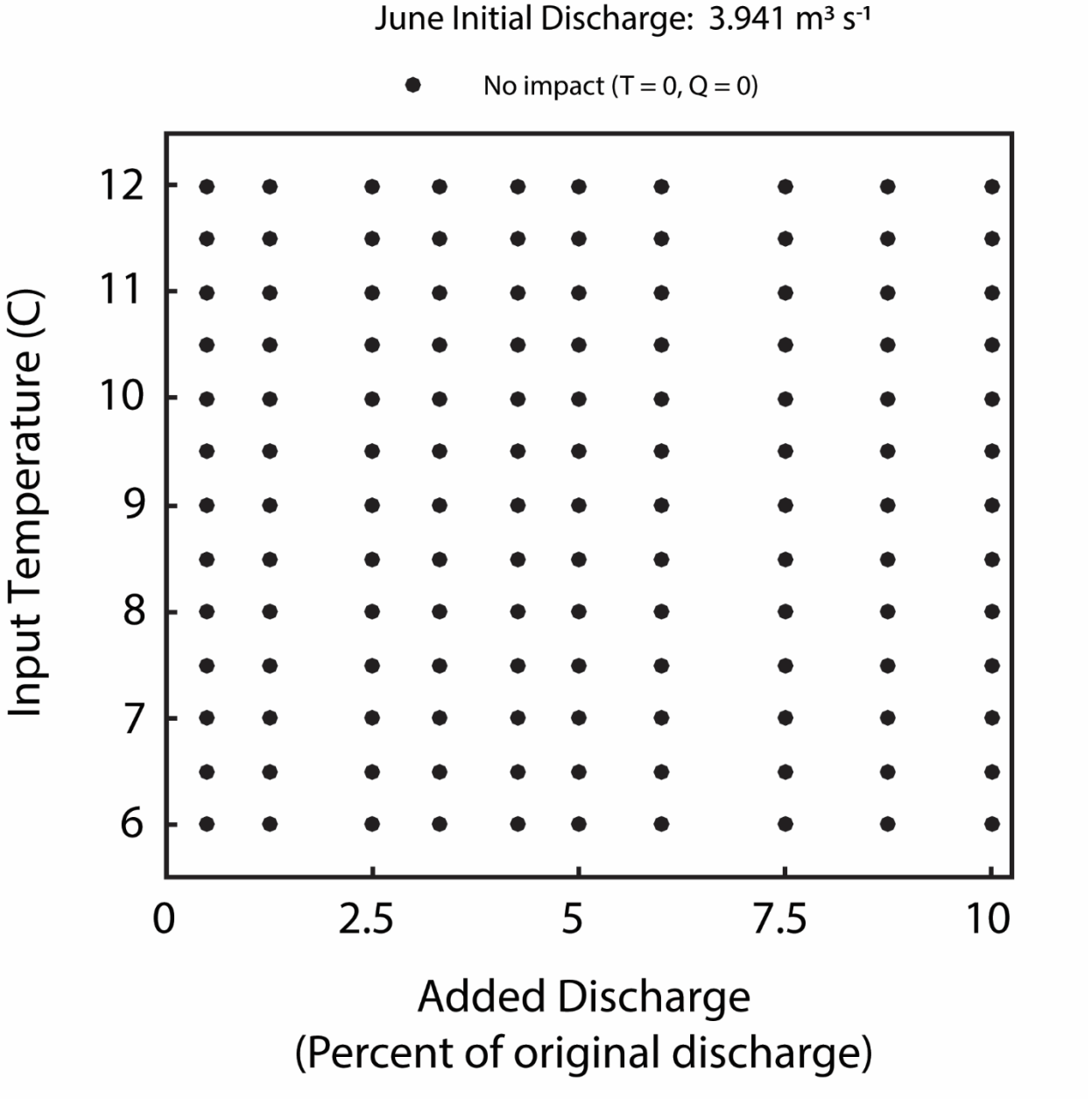

Figure A3: Shows the different combinations of storm water temperature (°C) and discharge (% of original discharge) for June. Each point represents one unique combination including a no impact run of no stormwater input. Original discharge is given above the figure.

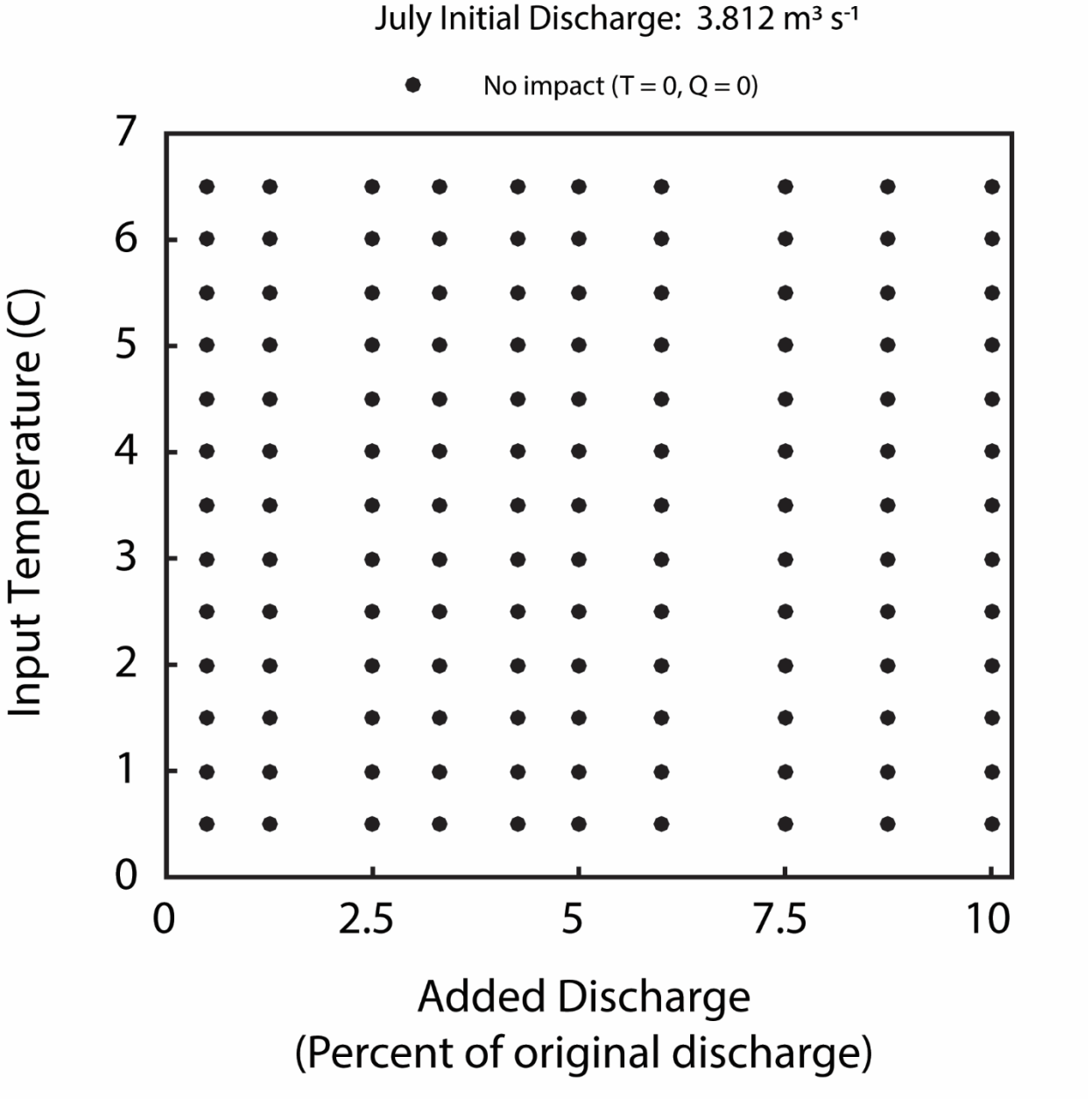

Figure A4: Shows the different combinations of storm water temperature (°C) and discharge (% of original discharge) for July. Each point represents one unique combination including a no impact run of no stormwater input. Original discharge is given above the figure.

Text A_3:

The following figure shows the relationship between increased discharge to Onondaga Creek and the stormwater temperatures at the drain in Site 4. We see that increased discharge does not lead to warmer stream temperatures, but find that instead, stormwater temperatures and discharge have an inverse relationship in Onondaga Creek.

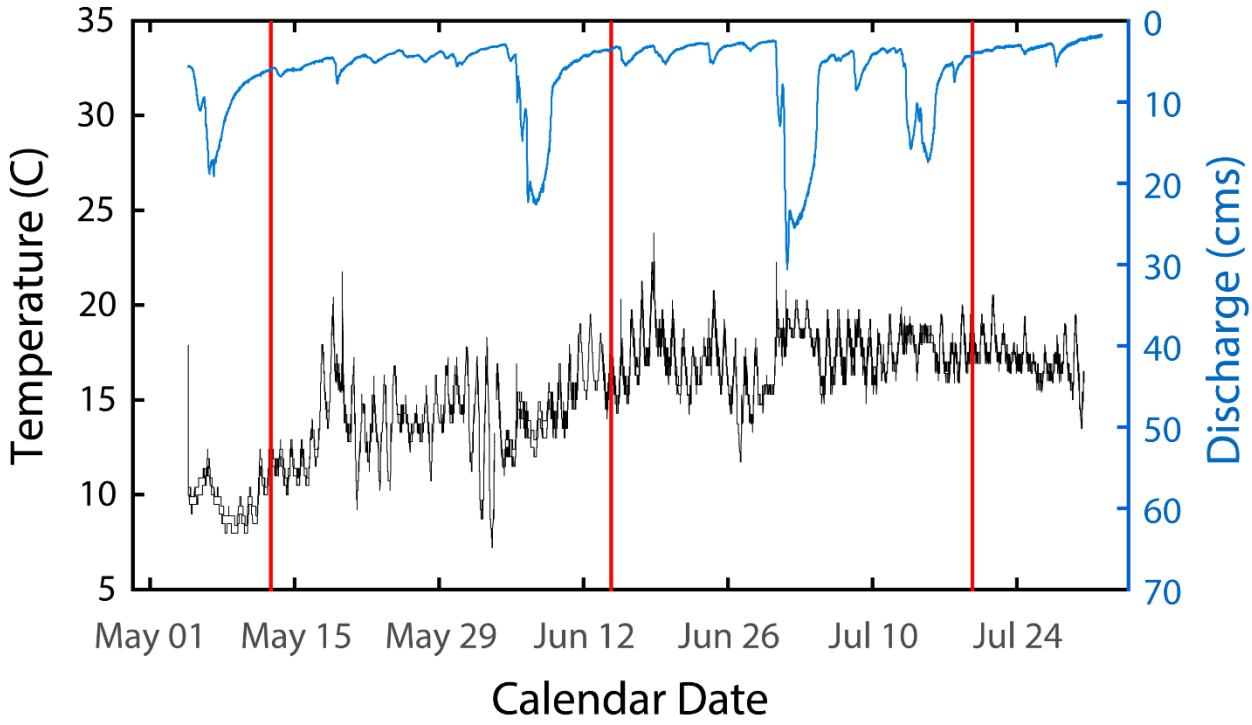

Figure A5: Shows the discharge in Onondaga Creek from May 4, 2017 to August 2, 2017 (blue), and the temperatures of stormwater input 2 (Site 4).

Text A_4:

Figures A_6 through A_{12} contain model results not shown in the manuscript.

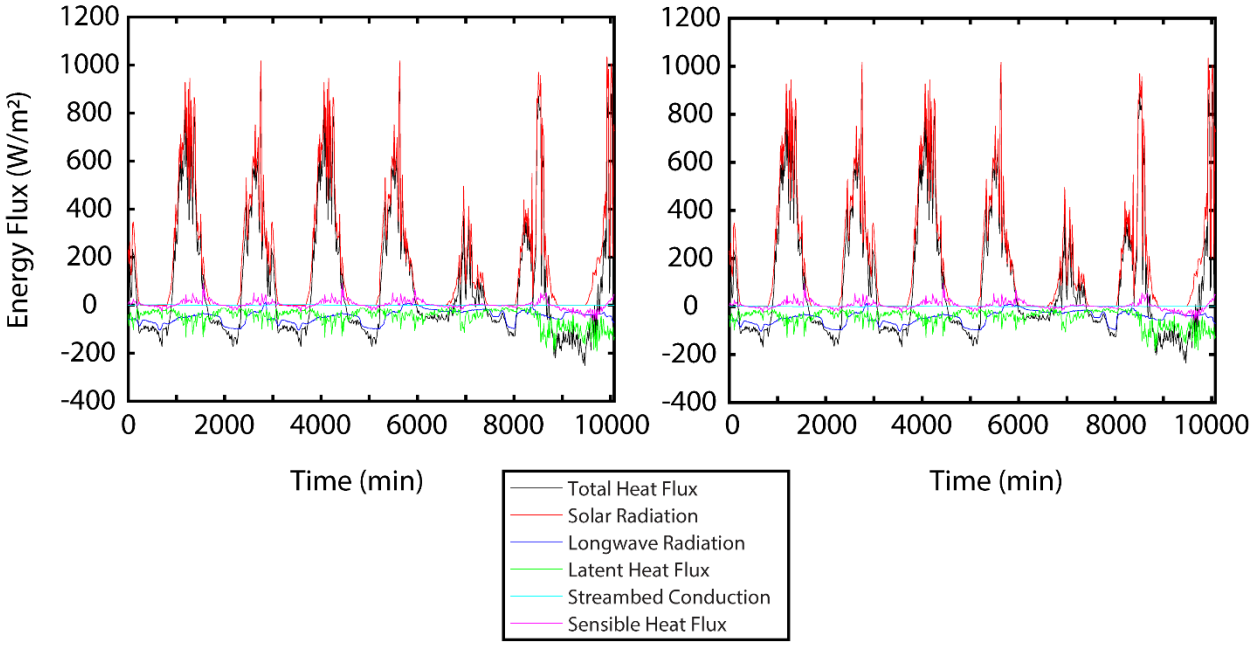

Figure A6: Shows the heat fluxes from the best fit temporally (left) and the run that met both spatial metrics with the lowest RMSE (right) for the May model scenarios.

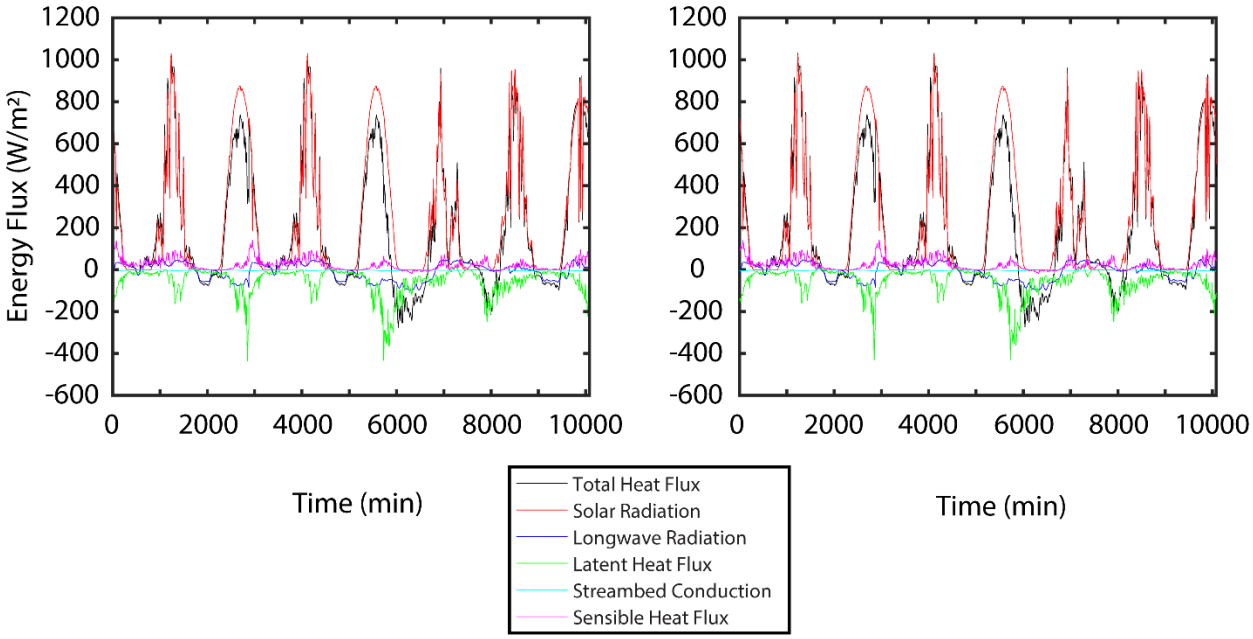

Figure A7: Shows the heat fluxes from the best fit temporally (left) and the run from those that met one of the spatial metrics with the lowest RMSE (right) for the June model scenarios as no runs met both spatial metrics.

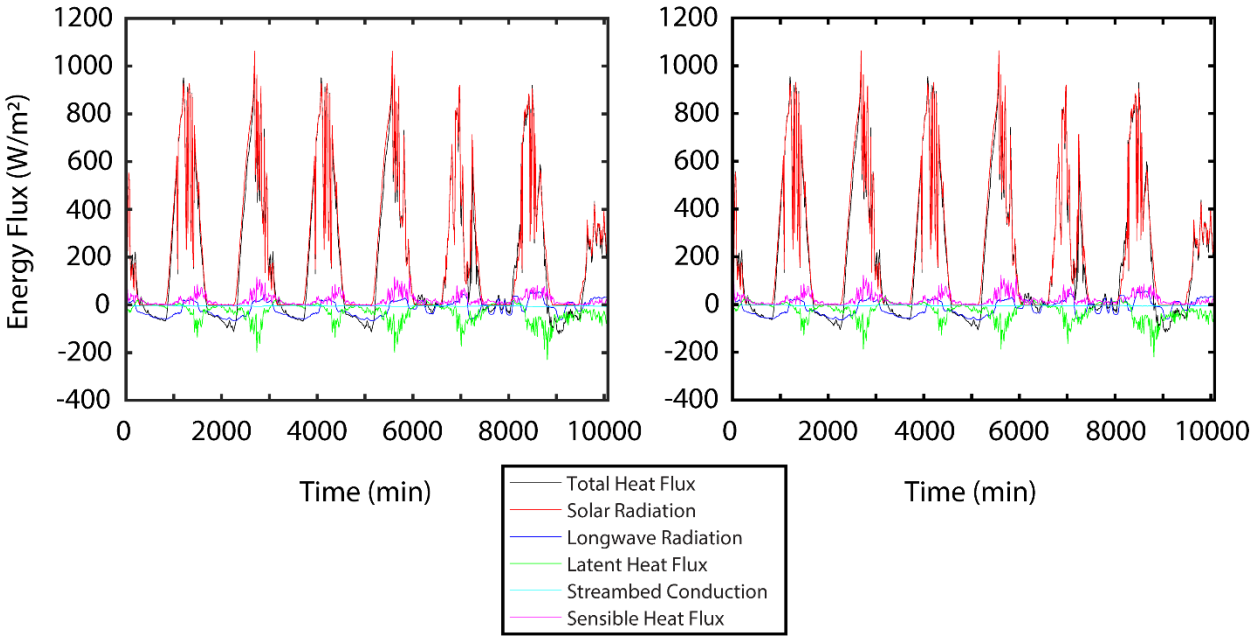

Figure A$_8$: Shows the heat fluxes from the best fit temporally (left) and the run that met both spatial metrics with the lowest RMSE (right) for the July model scenarios.

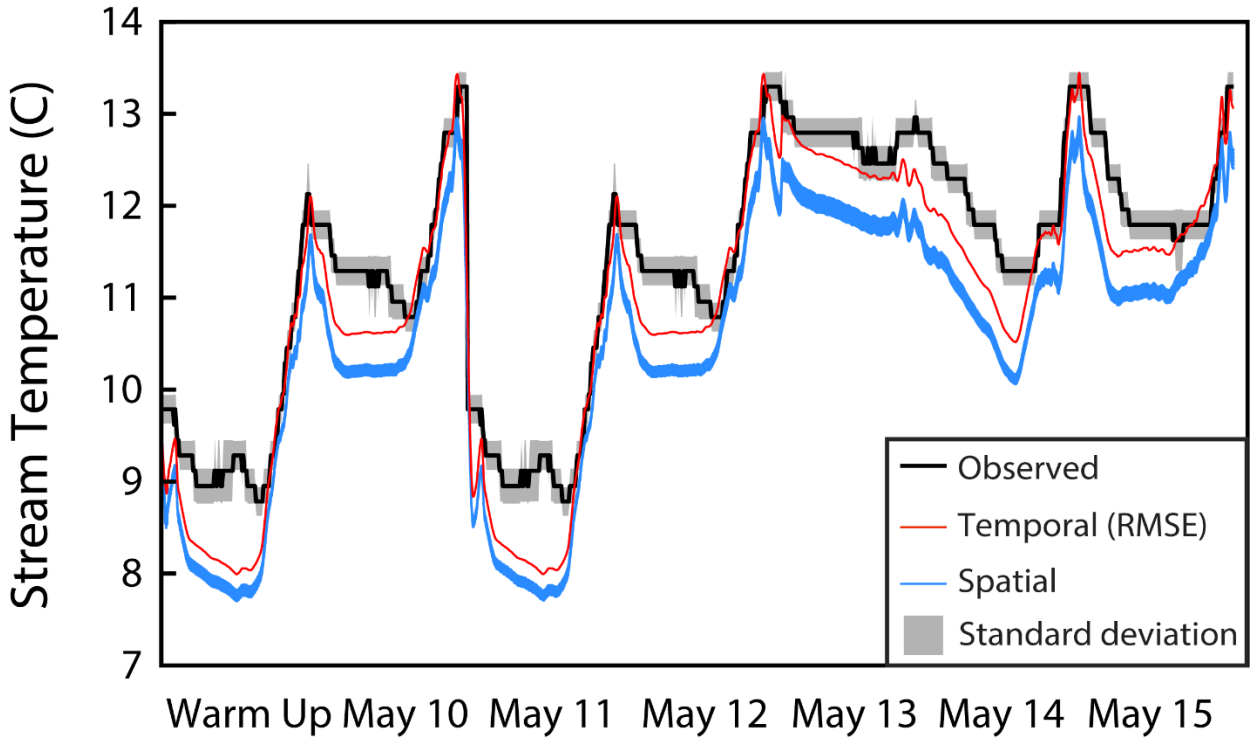

Figure A9: The average observed stream temperature timeseries (black) plotted alongside the six combinations of stormwater discharge and temperature that conformed to spatial metrics (red) and the simulation with the lowest RMSE (blue) for May modeling. The grey area represents the standards deviation of the iButton data.

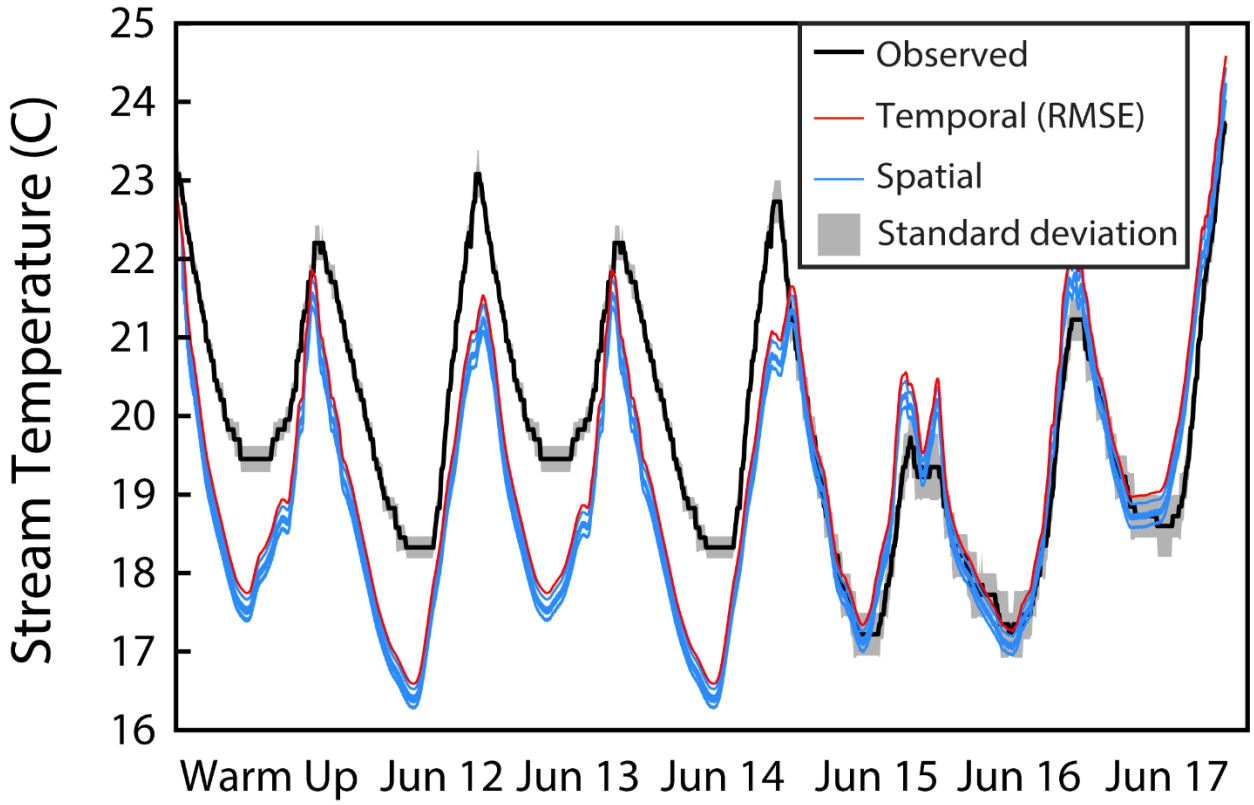

Figure A$_{10}$: The average observed stream temperature timeseries (black) plotted alongside the six combinations of stormwater discharge and temperature that conformed to spatial metrics (red) and the simulation with the lowest RMSE (blue) for June modeling. The grey area represents the standard deviation of the iButton data.

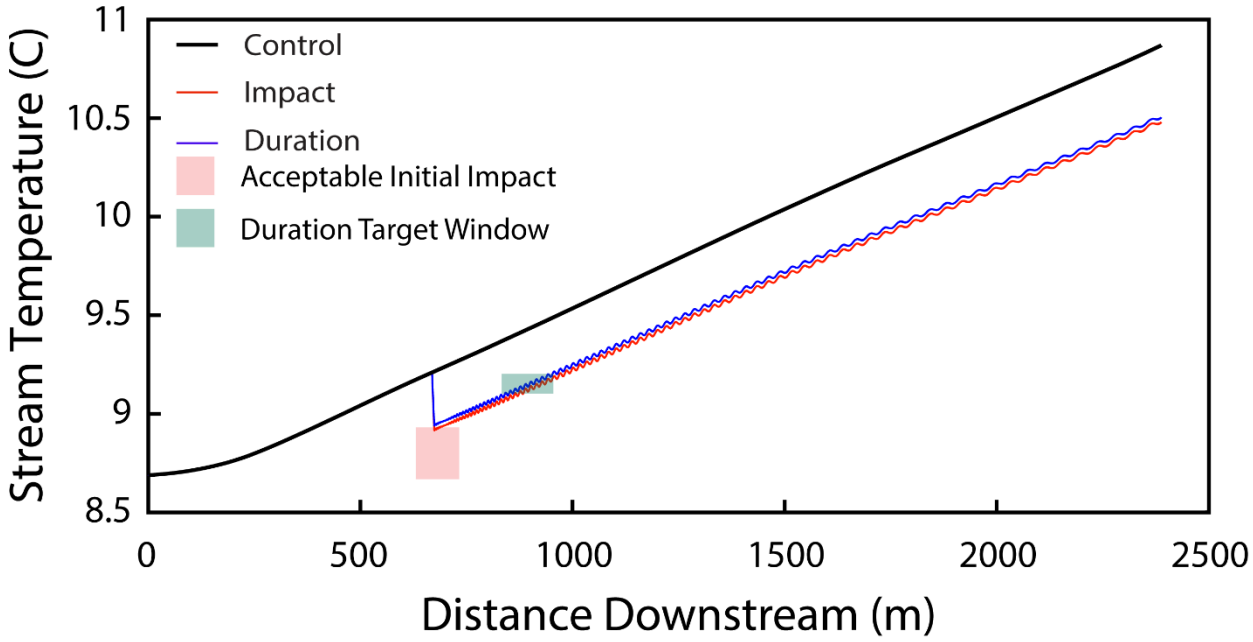

Figure A11: Distance series of the simulations with the best match for RMSE (black), Initial Impact (red) and Effect Duration (blue) for May simulations. 'Initial Impact' and 'Effect Duration' series correspond to a single simulation with the lowest RMSE that meets each of these spatial metrics. The red, and blue shaded areas represent the appropriate windows for Initial Impact and Effect Duration target window respectively. The target window is defined at the point at which stream temperature is within 0.1 °C of pre-stormwater stream temperature and falls within the corresponding month's acceptable duration window.

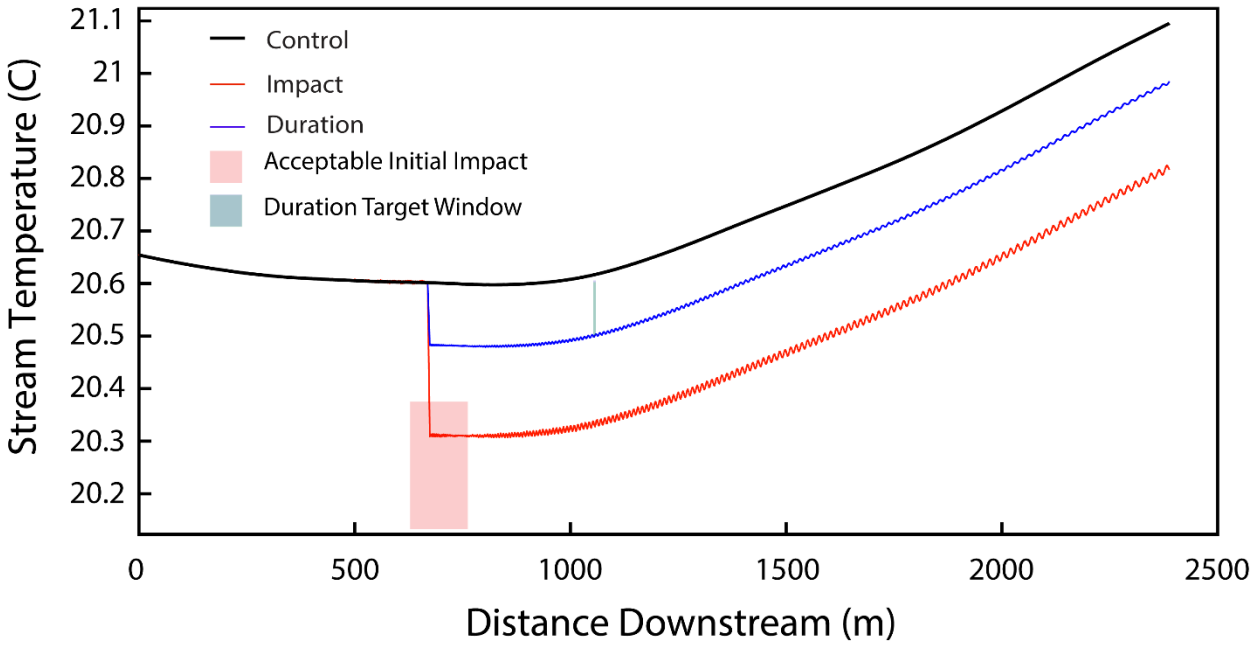

Figure A$_{12}$: Distance series of the simulations with the best match for RMSE (black), Initial Impact (red) and Effect Duration (blue) for June simulations. 'Initial Impact' and 'Effect Duration' series correspond to a single simulation with the lowest RMSE that meets each of these spatial metrics. The red, and blue shaded areas represent the appropriate windows for Initial Impact and Effect Duration target window respectively. The target window is defined at the point at which stream temperature is within 0.1 °C of pre-stormwater stream temperature and falls within the corresponding month's acceptable duration window.

9 References

Allan, J. David. *Stream Ecology: Structure and Function of Running Waters*. New York, NY. Springer. 1995

Bernot, Melody J., Daniel J. Sobota, Robert O. Hall, Patrick J. Mulholland, Walter K. Dodds, Jackson R. Webster, Jennifer L. Tank, et al. 2010. "Inter-Regional Comparison of Land-Use Effects on Stream Metabolism." *Freshwater Biology* 55 (9): 1874–90. doi:10.1111/j.1365-2427.2010.02422.x.

Beschta, Robert L. 1997. "Riparian Shade and Stream Temperature: An Alternative Perspective." *Rangelands* 19 (2): 25–28.

Buettner, K. J. K., and C. D. Kern. (1965). "The determination of infrared emissivities of terrestrial surfaces". *Journal of Geophysical Research.* 70 (6): 1329–1337. doi: 10.1029/JZ070i006p01329.

Bhan, R. K., R. S. Saxena, C. R. Jalwania, and S. K. Lomash. 2009. "Uncooled Infrared Microbolometer Arrays and Their Characterisation Techniques." *Defence Science Journal* 59 (6): 580–89. doi:10.14429/dsj.59.1562.

Booth, Derek B., Kristin A. Kraseski, and C. Rhett Jackson. 2014. "Local-Scale and Watershed-Scale Determinants of Summertime Urban Stream Temperatures." *Hydrological Processes* 28 (4): 2427–38. doi:10.1002/hyp.9810.

Caissie, D. 2006. "The Thermal Regime of Rivers: A Review." *Freshwater Biology* 51 (8): 1389–1406. doi:10.1111/j.1365-2427.2006.01597.x.

Cooper, Mendel. 2010. "Advanced Bash-Scripting Guide An in-Depth Exploration of the Art of Shell Scripting Table of Contents." *Okt 2005 Abrufbar Uber Httpwww Tldp orgLDPabsabsguide Pdf Zugriff 1112 2005* 2274 (November 2008): 2267–74. doi:10.1002/hyp.

Cooper, Mendel. 2010. "Advanced Bash-Scripting Guide An in-Depth Exploration of the Art of Shell Scripting Table of Contents." *Okt 2005 Abrufbar Uber Httpwww Tldp orgLDPabsabsguide Pdf Zugriff 1112 2005* 2274 (November 2008): 2267–74. doi:10.1002/hyp.

Dugdale, Stephen J. 2016. "A Practitioner's Guide to Thermal Infrared Remote Sensing of Rivers and Streams: Recent Advances, Precautions and Considerations." *Wiley Interdisciplinary Reviews: Water* 3 (April): 251–68. doi:10.1002/wat2.1135.

Fullerton, Aimee H., Christian E. Torgersen, Joshua J. Lawler, Russell N. Faux, E. Ashley Steel, Timothy J. Beechie, Joseph L. Ebersole, and Scott G. Leibowitz. 2015. "Rethinking the Longitudinal Stream Temperature Paradigm: Region-Wide Comparison of Thermal

Infrared Imagery Reveals Unexpected Complexity of River Temperatures." *Hydrological Processes* 29 (22): 4719–37. doi:10.1002/hyp.10506.

Garner, G., I. A. Malcolm, J. P. Sadler, and D. M. Hannah. 2014. "What Causes Cooling Water Temperature Gradients in a Forested Stream Reach?" *Hydrology and Earth System Sciences* 18 (12): 5361–76. doi:10.5194/hess-18-5361-2014.

Ghermandi, Andrea, Veronique Vandenberghe, Lorenzo Benedetti, Willy Bauwens, and Peter A. Vanrolleghem. 2009. "Model-Based Assessment of Shading Effect by Riparian Vegetation on River Water Quality." *Ecological Engineering* 35 (1): 92–104. doi:10.1016/j.ecoleng.2008.09.014.

Glose, Anne Marie, *Stream Heat Budget Modeling with the HFLUX Stream Temperature Solver: Model Development, Verification, and Applications*. Thesis, Syracuse University, 2013.

Glose, Anne Marie, and Laura K. Lautz. 2014. "Stream Heat Budget Modeling with HFLUX: Model Development, Verification, and Applications across Contrasting Sites and Seasons." *Environmental Modelling and Software* 92. Elsevier Ltd: 213–28. doi:10.1016/j.envsoft.2017.02.021.

Handcock, R. N., A. R. Gillespie, K. A. Cherkauer, J. E. Kay, S. J. Burges, and S. K. Kampf. 2006. "Accuracy and Uncertainty of Thermal-Infrared Remote Sensing of Stream Temperatures at Multiple Spatial Scales." *Remote Sensing of Environment* 100 (4): 427–40. doi:10.1016/j.rse.2005.07.007.

Handcock, Rebecca N., Christian E. Torgersen, Keith A. Cherkauer, Alan R. Gillespie, Klement Tockner, Russel N. Faux, and Jing Tan. 2012. "Thermal Infrared Remote Sensing of Water Temperature in Riverine Landscapes." *Fluvial Remote Sensing for Science and Management*, 85–113. doi:10.1002/9781119940791.ch5.

Hathaway, J. M., R. J. Winston, R. A. Brown, W. F. Hunt, and D. T. McCarthy. 2016. "Temperature Dynamics of Stormwater Runoff in Australia and the USA." *Science of the Total Environment* 559. Elsevier B.V.: 141–50. doi:10.1016/j.scitotenv.2016.03.155.

Hathway, E. A., and S. Sharples. 2012. "The Interaction of Rivers and Urban Form in Mitigating the Urban Heat Island Effect: A UK Case Study." *Building and Environment* 58. Elsevier Ltd: 14–22. doi:10.1016/j.buildenv.2012.06.013.

He, Li Ming (Lee), and Zhen Li He. 2008. "Water Quality Prediction of Marine Recreational Beaches Receiving Watershed Baseflow and Stormwater Runoff in Southern California, USA." *Water Research* 42 (10–11): 2563–73. doi:10.1016/j.watres.2008.01.002.

Herb, William R., Ben Janke, Omid Mohseni, and Heinz G. Stefan. 2008. "Thermal Pollution of Streams by Runoff from Paved Surfaces." *Hydrological Processes* 22 (7): 987–99. doi:10.1002/hyp.6986.

Holtby, L. Blair. 1988. “Effects of Logging on Stream Temperatures in Carnation Creek British Columbia, and Associated Impacts on the Coho Salmon (*Oncorhynchus Kisutch*).” *Canadian Journal of Fisheries and Aquatic Sciences* 45 (3): 502–15. doi:10.1139/f88-060.

Irvine, Dylan J., Martin A. Briggs, Laura K. Lautz, Ryan P. Gordon, Jeffrey M. Mckenzie, and Ian Cartwright. 2016. “Using Diurnal Temperature Signals to Infer Vertical Groundwater-Surface Water Exchange.” *Groundwater* 55 (1): 10–26. doi:10.1111/gwat.12459.

Irvine, Dylan J., and Laura K. Lautz. 2015. “High Resolution Mapping of Hyporheic Fluxes Using Streambed Temperatures: Recommendations and Limitations.” *Journal of Hydrology* 524. Elsevier B.V.: 137–46. doi:10.1016/j.jhydrol.2015.02.030.

Jensen A. M., B.T. Neilson, M. McKee, and Y. Chen. 2012. “Thermal remote sensing with an autonomous unmanned aerial remote sensing platform for surface stream temperatures”. *Geoscience and Remote Sensing Symposium (IGARSS), 2012 IEEE International*. 5049-5052. doi: 10.1109/IGARSS.2012.6352476

Kappel, William M, and Todd S Miller. 2005. “Hydrogeology of the Valley-Fill Aquifer in the Onondaga Trough , Onondaga County , New York”. US Geol Surv Sci Invest Rep 2005–5007.

Kirchner, J. W. 2006. “Getting the right answers for the right reasons: Linking measurements, analyses, and models to advance the science of hydrology”. *Water Resour. Res.* 42. W03S04. doi:10.1029/2005WR004362.

Kelleher, C., T. Wagener, M. Gooseff, B. McGlynn, K. McGuire, and L. Marshall. 2012. “Investigating Controls on the Thermal Sensitivity of Pennsylvania Streams.” *Hydrological Processes* 26 (5): 771–85. doi:10.1002/hyp.8186.

Lautz, Laura K., and Rachel E. Ribaudo. 2012. “Scaling up Point-in-Space Heat Tracing of Seepage Flux Using Bed Temperatures as a Quantitative Proxy.” *Hydrogeology Journal* 20 (7): 1223–38. doi:10.1007/s10040-012-0870-2.

Leach, J. A., and R. D. Moore. 2015. “Observations and Modeling of Hillslope Throughflow Temperatures in a Coastal Forested Catchment.” *Water Resources Research*, 3770–95. doi:10.1002/2014WR016763.

Lebosquet, M, and E C Tsivoglou. 2017. “Simplified Dissolved Oxygen Computations”. *Water Environment Federation* 22 (8): 1054–61.. http://www.jstor.org/stable/25031370

Lee, Eunhee, Heesung Yoon, Sung Pil Hyun, William C. Burnett, Dong Chan Koh, Kyoochul Ha, Duk Jin Kim, Yongcheol Kim, and Ki Mook Kang. 2016b. “Unmanned Aerial Vehicles (UAVs)-Based Thermal Infrared (TIR) Mapping, a Novel Approach to Assess Groundwater Discharge into the Coastal Zone.” *Limnology and Oceanography: Methods* 14 (11): 725–35. doi:10.1002/lom3.10132.

LeBlanc, R T, R D Brown, and J E FitzGibbon. 1997. “Modeling the Effects of Land Use Change on the Water Temperature in Unregulated Urban Streams.” *Journal of Environmental Management* 49: 445–69. doi:10.1006/jema.1996.0106.

Likens, Gene E., F. Herbert Bormann, Noye M. Johnson, D. W. Fisher, and Robert S. Pierce. 1970. “Effects of Forest Cutting and Herbicide Treatment on Nutrient Budgets in the Hubbard Brook Watershed-Ecosystem.” *Ecological Monographs* 40 (1): 23–47. doi:10.2307/1942440.

Liu, Chuankun, Jie Liu, Yue Hu, Heshun Wang, and Chunmiao Zheng. 2016. “Airborne Thermal Remote Sensing for Estimation of Groundwater Discharge to a River.” *Groundwater* 54 (3): 363–73. doi:10.1111/gwat.12362.

Mallick, K. , Toivonen, E. , Trebs, I. , Boegh, E. , Cleverly, J. , Eamus, D. , Koivusalo, H. , Drewry, D. , Arndt, S. K., Griebel, A. , Beringer, J. and Garcia, M. (2018), “Bridging Thermal Infrared Sensing and Physically-Based Evapotranspiration Modeling: From Theoretical Implementation to Validation Across an Aridity Gradient in Australian Ecosystems”. *Water Resour. Res.*. Accepted Author Manuscript. doi:10.1029/2017WR021357

Nelson, Kären C., and Margaret A. Palmer. 2007. “Stream Temperature Surges under Urbanization and Climate Change: Data, Models, and Responses.” *Journal of the American Water Resources Association* 43 (2): 440–52. doi:10.1111/j.1752-1688.2007.00034.x.

Niklaus, Frank, Adit Decharat, Christer Jansson, and Göran Stemme. 2008. “Performance Model for Uncooled Infrared Bolometer Arrays and Performance Predictions of Bolometers Operating at Atmospheric Pressure.” *Infrared Physics and Technology* 51 (3): 168–77. doi:10.1016/j.infrared.2007.08.001.

Nishar, Abdul, Steve Richards, Dan Breen, John Robertson, and Barbara Breen. 2016. “Thermal Infrared Imaging of Geothermal Environments and by an Unmanned Aerial Vehicle (UAV): A Case Study of the Wairakei - Tauhara Geothermal Field, Taupo, New Zealand.” *Renewable Energy* 86. Elsevier Ltd: 1256–64. doi:10.1016/j.renene.2015.09.042.

Olden, Julian D., and Robert J. Naiman. 2010. “Incorporating Thermal Regimes into Environmental Flows Assessments: Modifying Dam Operations to Restore Freshwater Ecosystem Integrity.” *Freshwater Biology* 55 (1): 86–107. doi:10.1111/j.1365-2427.2009.02179.x.

Owens, Emmet M., Steven W. Effler, David M. O’Donnell, and David A. Matthews. 2014. “Modeling the Fate and Transport of Plunging Inflows to Onondaga Lake.” *Journal of the American Water Resources Association* 50 (1): 205–18. doi:10.1111/jawr.12130.

Poole, GEOFFREY C., and CARA H. Berman. 2001. “An Ecological Perspective on in-Stream Temperature: Natural Heat Dynamics and Mechanisms of Human-Caused Thermal Degradation.” *Environmental Management* 27 (6): 787–802. doi:10.1007/s002670010188.

Rautio, A., A. L. Kivimäki, K. Korkka-Niemi, M. Nygård, V. P. Salonen, K. Lahti, and H. Vahtera. 2015. "Vulnerability of Groundwater Resources to Interaction with River Water in a Boreal Catchment." *Hydrology and Earth System Sciences* 19 (7): 3015–32. doi:10.5194/hess-19-3015-2015.

Rossi, L, and R E Hari. 2007. "Screening Procedure to Assess the Impact of Urban Stormwater Temperature to Populations of Brown Trout in Receiving Water." *Integrated Environmental Assessment and Management* 3 (3): 383–92. pdf. doi: 10.1897/1551-3793(2007)3[383:SPTATI]2.0.CO;2

Sabouri, F., B. Gharabaghi, A. A. Mahboubi, and E. A. McBean. 2013. "Impervious Surfaces and Sewer Pipe Effects on Stormwater Runoff Temperature." *Journal of Hydrology* 502. Elsevier B.V.: 10–17. doi:10.1016/j.jhydrol.2013.08.016.

Sabouri, F., B. Gharabaghi, A. M A Sattar, and A. M. Thompson. 2016. "Event-Based Stormwater Management Pond Runoff Temperature Model." *Journal of Hydrology* 540. Elsevier B.V.: 306–16. doi:10.1016/j.jhydrol.2016.06.017.

Schindler, D W. 2001. "The Cumulative Effects of Climate Warming and Other Human Stresses on Canadian Freshwaters in the New Millennium." *Canadian Journal of Fisheries and Aquatic Sciences* 58 (1): 18–29. doi:10.1139/f00-179.

Schmadel, Noah M., Bethany T. Neilson, and Tamao Kasahara. 2014. "Deducing the Spatial Variability of Exchange within a Longitudinal Channel Water Balance." *Hydrological Processes* 28 (7): 3088–3103. doi:10.1002/hyp.9854.

Seibert, J., and J. J. McDonnell. 2002. 'On the dialog between experimentalist and modeler in catchment hydrology: Use of soft data for multicriteria model calibration". *Water Resour. Res.*. 38(11): 1241. doi:10.1029/2001WR000978, 2002.

Somers, Kayleigh a., Emily S. Bernhardt, James B. Grace, Brooke A. Hassett, Elizabeth B. Sudduth, Siyi Wang, and Dean L. Urban. 2013. "Streams in the Urban Heat Island: Spatial and Temporal Variability in Temperature." *Freshwater Science* 32 (1): 309–26. doi:10.1899/12-046.1.

Sun, Ning, John Yearsley, Nathalie Voisin, and Dennis P. Lettenmaier. 2015. "A Spatially Distributed Model for the Assessment of Land Use Impacts on Stream Temperature in Small Urban Watersheds." *Hydrological Processes* 29 (10): 2331–45. doi:10.1002/hyp.10363.

Thompson, A. M., T. Wilson, J. M. Norman, A. L. Gemechu, and A. Roa-Espinosa. 2008. "Modeling the Effect of Summertime Heating on Urban Runoff Temperature." *Journal of the American Water Resources Association* 44 (6): 1548–63. doi:10.1111/j.1752-1688.2008.00259.x.

Torgersen, Ce, and Jl Ebersole. 2012. “Primer for Identifying Cold-Water Refuges to Protect and Restore Thermal Diversity in Riverine Landscapes.” *EPA Scientific Guidance Handbook*, no. February: 91. doi:EPA 910-c-12-001.

Van Buren, M. A. Van, W. E. Watt, J. Marsalek, and B. C. Anderson. 2000. “Thermal Enhancement of Stormwater Runoff by Paved Surfaces.” *Water Research* 34 (4): 1359–71. doi:10.1016/S0043-1354(99)00244-4.

Walsh, Christopher J, Allison H Roy, Jack W Feminella, Peter D Cottingham, Peter M Groffman, and Raymond P Morgan. 2005. “The Urban Stream Syndrome: Current Knowledge and the Search for a Cure.” *Journal of the North American Benthological Society* 24 (3): 706. doi:10.1899/0887-3593(2005)024\[0706:TUSSCK\]2.0.CO;2.

Wang, L, and P Kanehl. 2003. “Influences of Watershed Urbanization and Instream Habitat on Macroinvertebrates in Cold Water Streams.” *Journal of the American Water Resources Association* 39 (5): 1181–96. doi:10.1111/j.1752-1688.2003.tb03701.x.

Webb, BW. 1996. “Trends in Stream and River Temperature.” *Hydrological Processes* 10 (June 1994): 205–26. doi:10.1002/(SICI)1099-1085(199602)10:2<205::AID-HYP358>3.0.CO;2-1.

Wenger, S J, A H Roy, C R Jackson, E S Bernhardt, T L Carter, S Filoso, C A Gibson, et al. 2009. “Twenty-Six Key Research Questions in Urban Stream Ecology: An Assessment of the State of the Science.” *J. N. Am. Benthol. Soc.* 28 (4): 1080–98. doi:Doi 10.1899/08-186.1.

Westhoff, M, H Savenije, W Luxemburg, G S Stelling, N C van de Giesen, J S Selker, L Pfister, and S Uhlenbrook. 2007. “A Distributed Stream Temperature Model Using High Resolution Temperature Observations.” *Hydrology and Earth System Sciences* 11: 1469–80. doi:10.5194/hessd-4-125-2007.

Whitehead, P. G., R. L. Wilby, R. W. Battarbee, M. Kernan, and A. J. Wade. 2009. “A Review of the Potential Impacts of Climate Change on Surface Water Quality.” *Hydrological Sciences Journal* 54 (1): 101–21. doi:10.1623/hysj.54.1.101.

Wu, Jing-Hong. 2014. “Effect of Ground Covers on Soil Temperature in Urban and Rural Areas.” *Environmental & Engineering Geoscience* 20 (3): 225–37.

Yager, Richard M., William M. Kappel, and L. Niel Plummer. 2007. “Origin of Halite Brine in the Onondaga Trough near Syracuse, New York State, USA: Modeling Geochemistry and Variable-Density Flow.” *Hydrogeology Journal* 15 (7): 1321–39. doi:10.1007/s10040-007-0186-9.

Yokobori, Takuya, and Shunji Ohta. 2009. “Effect of Land Cover on Air Temperatures Involved in the Development of an Intra-Urban Heat Island.” *Climate Research* 39 (1): 61–73. doi:10.3354/cr00800.

Zeiger, Sean, and Jason Hubbart. 2015. “Urban Stormwater Temperature Surges: A Central US Watershed Study.” *Hydrology* 2 (4): 193–209. doi:10.3390/hydrology2040193.

Samuel H. Caldwell

300 S. 11th St #3124 ● Richmond, VA 23219 ● (704) 608-3453 ● sam.caldwell93@gmail.com

Education, Honors & Awards

Aug 2016- May 2018 **SYRACUSE UNIVERSITY** Syracuse, NY

Candidate for M.S. in Geoscience expected June 2018

- EMPOWER NRT Trainee
- EMPOWER NRT Fellowship recipient (Aug 2017-Jul 2018)

Aug 2012- May 2016 **AMHERST COLLEGE** Amherst, MA

B.A. in Geology May 2016

- Associate Member of the Amherst College Chapter of Sigma Xi Class of 2016
- Recipient of The John Mason Clarke 1877 Fellowship in Paleontology and Geology (April 2016)

Oct 2017 **3rd Place Master's Degree Category** Syracuse, NY

- Awarded the third-place prize in the Masters Degree category of the Student Poster Competition at the 17th Annual Syracuse Center of Excellence Symposium.

Key Skills

Hydrology, Hydrogeology, Matlab, R, ArcGIS, Python, Java, critical thinking, statistical analysis, technical writer, Microsoft Word, Microsoft Excel, Dual citizen with Ireland and USA, Level 1 Thermography certification

Experience

Aug 2016- May 2017 **SYRACUSE UNIVERSITY EARTH SCIENCE DEPARTMENT** Syracuse, NY

Masters Thesis Student; Teaching Assistant: Earth Sciences 104, 106, and 110

- Examined the effect of culverted inputs on stream temperature and variance in urban streams using TIR and UAVs in pursuit of a M.S. thesis.
- Presented Posters at Syracuse CoE Symposium 2017 and GSA 2017 (Seattle, WA)
- Designed and taught labs to undergraduate students for three Earth Science courses teaching the principles of Earth Science to students using a variety of visual and lecture-based methods

Jun 2015- May 2016 **KECK GEOLOGY CONSORTIUM** Newberry, OR; Middletown, CT; Amherst, MA

Student Researcher: Crater Lakes, OR Project

- April 2016 Researched the nutrients, archaea, and methane of East and Paulina Lake using water and nutrient profiles, isotope ratios, and methane isotope systematics
- Presented posters at the 2016 KECK Conference 2016 Northeastern GSA

Athletics

Aug 2012- Nov2015 **AMHERST COLLEGE FOOTBALL PROGRAM** Amherst, MA

Defensive lineman

- Developed skills for working efficiently in large and small teams
- Improved individually through self-analysis to identify and fix mistakes in real time

Personal

12 years (ongoing) playing the oboe